Transfer Report

submitted by Jack C. H. Blake

as part of a Ph. D. sponsored by AMEC

at the University of Bath

Contents

Chapter 1

Introduction to the Neutron Transport Equation

1.1 The Neutron Transport Equation in 3D

An important problem in applied nuclear physics is that of efficiently solving the neutron transport equation. This equation governs the behaviour of neutrons within a nuclear fission reaction by specifying a quantity known as the *neutron flux*, which we denote $\psi(\mathbf{r}, \Omega, E)$, where $\mathbf{r} \in V \subset \mathbb{R}^3$ is the neutron's location in a 3D coordinate system, $\Omega \in \mathbb{S}^2$ is its direction of travel, and $E \in \mathbb{R}^+$ is the neutron's kinetic energy. The quantity $\psi(\mathbf{r}, \Omega, E)$ is then the number of neutrons passing through a unit space at $\mathbf{r}$ in direction Ω with energy E per unit time. The transport equation describes the behaviour of the neutron flux based upon the likelihood of various neutron interactions (or collisions) occurring, and based on the characteristics of a *neutron source*. Throughout this document we will be considering only steady-state versions of the neutron transport equation, so there will be no time dependence.

When modelling a nuclear reactor, it is generally specified that neutrons can undergo three types of interaction: they can cause *fission*, can be *scattered* or they can be *captured*. Neutron-neutron interactions are not often considered due to the small size of a neutron, and thus the comparative improbability of these events. We consider the three interactions in order.

First of all, a neutron could collide with some *fissile material* and undergo a *fission event*. Fissile material is material which, upon collision with a low-energy (*slow* or *thermal*) neutron, can capture it and then undergo a fission event [28]. This releases a number of new neutrons, specified by $\nu(E) \in \mathbb{R}^+$ for a collision caused by a neutron with energy E. These are released over a spectrum of different energies specified by $\chi(E) \in \mathbb{R}^+$, where $\chi(E)\mathrm{d}E$ is the probability that a neutron produced during fission will have an energy within $\mathrm{d}E$ of E [20]. The neutrons produced by the fission may

be travelling in any direction with no bias (i.e. they are *isotropic* in angle). This is a *fission collision* and the likelihood of such a collision occurring is denoted by the variable $\sigma_F(\mathbf{r}, E) \in \mathbb{R}^+$, known as the *fission cross-section*.

Next, upon collision with a nucleus, a neutron could be deflected and so end up travelling in a different direction with different energy. In this case the neutron is said to have been *scattered* and the likelihood of such an event occurring is denoted by the variable $\sigma_S(\mathbf{r}, \Omega' \cdot \Omega, E', E) \in \mathbb{R}^+$, known as the *scatter cross-section*. Here the neutron is scattered from travelling with energy E' in direction Ω' to travelling with energy E in direction Ω.

Lastly, upon collision with a nucleus a neutron could be *captured* and so no longer be considered within the ongoing reaction. The likelihood of such an event occurring is denoted by the variable $\sigma_C(\mathbf{r}, E) \in \mathbb{R}^+$ and is known as the *capture cross-section*. If we denote by $\sigma_T(\mathbf{r}, E) \in \mathbb{R}^+$ a quantity known as the *total cross-section*, defined to be the likelihood of any collision occurring to neutrons at position $\mathbf{r}$ with energy E, then the following relation holds

$$\sigma_T(\mathbf{r}, E) = \sigma_F(\mathbf{r}, E) + \int_{\mathbb{R}^+} \int_{\mathbb{S}^2} \sigma_S(\mathbf{r}, \Omega' \cdot \Omega, E', E) \, \mathrm{d}\Omega' \, \mathrm{d}E' + \sigma_C(\mathbf{r}, E). \tag{1.1}$$

We will also define for convenience $\sigma_A(\mathbf{r}, E) \equiv \sigma_C(\mathbf{r}, E) + \sigma_F(\mathbf{r}, E)$. This is called the *absorption* cross-section, and represents all collisions which result in the neutron being absorbed.

It is important to note that since $\psi(\mathbf{r}, \Omega, E)$ only considers specific angles and energies, after each of the three collision types the neutron is no longer travelling in the same direction with the the same energy, and so is no longer a part of that specific neutron flux. The *neutron source* term will be denoted by $Q(\mathbf{r}, E)$ and is a non-fission source term of neutrons from position $\mathbf{r}$ with energy E in all directions. While this source could include angular dependency also, most natural source materials are isotropic in angle and so ignoring it is still very physically relevant, and avoids adding unnecessary confusion.

Using this notation we can now state the 3D steady-state neutron transport equation as follows

$$\begin{aligned}\Omega \cdot \nabla\psi(\mathbf{r},\Omega,E) \; + \; \sigma_T(\mathbf{r},E)\psi(\mathbf{r},\Omega,E) \; = \\ & \int_{\mathbb{R}^+}\int_{\mathbb{S}^2} \sigma_S(\mathbf{r},\Omega'\cdot\Omega,E',E)\psi(\mathbf{r},\Omega',E')\,\mathrm{d}\Omega'\,\mathrm{d}E' \\ & + \; \frac{\chi(E)}{4\pi}\int_{\mathbb{R}^+}\nu(\mathbf{r},E')\sigma_F(\mathbf{r},E')\int_{\mathbb{S}^2}\psi(\mathbf{r},\Omega',E')\,\mathrm{d}\Omega'\,\mathrm{d}E' \\ & + \; Q(\mathbf{r},E),\end{aligned} \tag{1.2}$$

for $(\mathbf{r},\Omega,E) \in V \times \mathbb{S}^2 \times \mathbb{R}^+$. The terms on the left of (1.2) represent neutron loss from the system, while the other three terms represent neutron gain. We will now briefly talk through their physical meanings. The first term on the left represents neutron loss due to streaming, while the second term removes those neutrons that undergo any type of collision. The first term on the right adds in those neutrons which have been scattered from other energies and/or directions (E' and Ω') into the considered energy and direction (E and Ω), and so are now to be considered a part of the flux. The second term adds neutrons that have been produced by nuclear fission, travelling in the correct direction with the correct energy. Finally $Q(\mathbf{r},E)$ adds in neutrons produced by the non-fission source.

This equation plays an important role in many different applications of nuclear reactors across an array of disciplines. These range from medical applications (such as the production of radio-isotopes and radiation therapy), through propulsion methods for ships and also its most well known application in nuclear power stations producing electricity [28]. Outside of nuclear reactors it is also solved in shielding calculations (see [23] Section 2.11.4, and elsewhere in [8]), such as are used for ensuring adequate safety measures around x-ray machines in hospitals. To fulfil these needs, a wide array of industrial modelling codes rely upon efficient and accurate solutions of the neutron transport equation. The transport equation, (1.2), is six-dimensional, which necessitates the use of iterative methods to achieve accurate solutions within a reasonable amount of time. As a result much interest and ongoing research is focussed around improving the efficiency of these iterative methods, and it is on this topic that our work is based.

1.1.1 Simplifying Assumptions

Throughout this report several physical assumptions will be made in order to reduce the transport equation into a form that is simpler to analyse. It has already been mentioned that we are considering the steady-state form of the neutron transport equation, which is why no time dependence was introduced in the previous section. We will further assume that all neutrons are travelling with the same energy, thus removing this

dependence from all areas of consideration. This is not a realistic assumption since in reality the energy a particle has dramatically affects the cross-sections. In fact, the variation of the cross-sections with respect to a neutron's energy is so complex that it cannot be calculated or accurately modelled at each point, so instead a range of energy 'intervals' (or 'groups') are considered (see [20], [27]). In this regard, we will be using just one interval in our model. This is often referred to as working in the *monoenergetic* case. As a consequence we must also assume that neutron collisions occur without energy loss. Despite the dramatic nature of this assumption, the monoenergetic transport equation is frequently considered since it allows more rigorous mathematical analysis [23] (Section 2.9).

We will assume that the scattering cross-section is independent of angle. To establish this independence, we must write $\sigma_S()$ as an expansion in Legendre polynomials, which are defined via Rodrigues' formula as

$$P_n(\mu) = \frac{1}{2^n n!} \frac{\mathrm{d}^n}{\mathrm{d}\mu^n} \left(\mu^2 - 1\right)^n, \quad n \in \mathbb{N}_0. \tag{1.3}$$

Using these, the monoenergetic scattering cross section can be expanded as

$$\sigma_S(\mathbf{r}, \Omega' \cdot \Omega) = \sum_{n=0}^{N} \frac{2n+1}{4\pi} \sigma_{S,n}(\mathbf{r}) P_n(\Omega' \cdot \Omega), \tag{1.4}$$

(see [23] Section 3.1). In most applications this expansion is truncated, and if $N = 0$ is chosen then the scattering is said to be *isotropic*. This leaves

$$\sigma_S(\mathbf{r}) = \frac{1}{4\pi} \sigma_{S,0}(\mathbf{r}), \tag{1.5}$$

however since this report will be solely focussed on the case of isotropic scattering, we will simply use the notation σ_S.

As well as this we will assume that all cross-sections are independent of space. This assumption implies that we are working within a homogeneous medium, and that there are no material boundaries within our domain of interest.

Under these assumptions the transport equation (1.2) becomes

$$\Omega \cdot \nabla \psi(\mathbf{r}, \Omega) + \sigma_T \psi(\mathbf{r}, \Omega) = \frac{\sigma_S}{4\pi} \int_{\mathbb{S}^2} \psi(\mathbf{r}, \Omega') \, \mathrm{d}\Omega' + Q(\mathbf{r}). \tag{1.6}$$

for $(\mathbf{r}, \Omega) \in V \times \mathbb{S}^2$. In this we have also not included the term relating to fission interactions. This may appear to be a big assumption to make, however the fission term can be thought to have been included implicitly in the scatter term. Hence our later analysis will apply to both the with fission and without fission cases.

1.1.2 Boundary Conditions

As with any differential equation, (1.6) can only be solved when combined with some relevant boundary conditions. We will consider two types of condition in this section: *vacuum* boundary conditions and *reflecting* boundary conditions.

First of all, vacuum conditions are used to enforce a requirement for zero incoming neutron flux over the boundary of the spatial domain. This means that the only source of neutrons under consideration is from within the reactor itself. To enforce this, we specify that the neutron flux, ψ, satisfies

$$\psi(\mathbf{r}, \Omega) = 0 \quad \text{when } n(\mathbf{r}) \cdot \Omega < 0, \ \ \forall \mathbf{r} \in \delta V \tag{1.7}$$

where $n(\mathbf{r})$ is the outward unit vector, normal to the surface δV at $\mathbf{r}$. So we have that at all points on the boundary of the domain ($\mathbf{r} \in \delta V$), the neutron flux in the inward direction is zero.

Next, reflecting boundary conditions say that the incoming flux and outgoing flux at the boundary of the spatial domain are equal. These conditions can be specified as follows. For all points $(\mathbf{r}, \Omega_1) \in \delta V \times \mathbb{S}^2$, define the *local reflection* to be the reflection of Ω_1 in the tangent plane of δV at $\mathbf{r}$. If Ω_2 is the local reflection of Ω_1, then

$$\psi(\mathbf{r}, \Omega_1) = \psi(\mathbf{r}, \Omega_2). \tag{1.8}$$

This ensures that the boundary flux in an outgoing angle equals that of the reflected incoming angle at each point on the boundary of the domain. This prevents neutrons from escaping the system, instead *reflecting* them back inwards. In more complicated geometries, these can be used to model infinite arrays of a certain region. This is done by defining one copy of the region, and then applying reflecting conditions around the boundary. This implicitly assumes an average flux of zero over boundaries between the regions, however can still be a good representation of the set up.

Throughout this report we will use vacuum boundary conditions, (1.7), in conjunction with the transport equation (1.6). At relevant points we will specify this again to ensure there is no confusion.

To allow mathematical rigour in our later analysis, we shall specify the space we are working within. Define

$$L^2\left(V, L^1(\mathbb{S}^2)\right) \equiv \left\{ \psi : V \times \mathbb{S}^2 \to \mathbb{R} \ : \ \int_V \|\psi(\mathbf{r}, \cdot)\|^2_{L^1(\mathbb{S}^2)} \ \mathrm{d}\mathbf{r} < \infty \right\},$$

where

$$\|\psi\|^2_{L^2(V, L^1(\mathbb{S}^2))} = \int_V \|\psi(\mathbf{r}, \cdot)\|^2_{L^1(\mathbb{S}^2)} \ \mathrm{d}\mathbf{r},$$

and

$$\|\psi(\mathbf{r},\cdot)\|_{L^1(\mathbb{S}^2)} \equiv \int_{\mathbb{S}^2} |\psi(\mathbf{r},\Omega)| \, \mathrm{d}\Omega,$$

is the usual L^1-norm. With this we can say that during this report, in solving (1.6) we are looking for some $\psi \in L^2\left(V, L^1(\mathbb{S}^2)\right)$ that satisfies vacuum boundary conditions, (1.7), with $\nabla \cdot \psi \in L^2\left(V, L^1(\mathbb{S}^2)\right)$ also.

1.1.3 Operator Form

To simplify the expression of transport equation (1.6) we will now introduce three operators ($\mathcal{T}$, $\mathcal{S}$ and $\mathcal{P}$) which will prove highly useful during this report. The first two respresent the *transport* and *scatter* parts of the transport equation respectively, and are defined as follows

$$\begin{aligned} \mathcal{T}(\cdot) &\equiv \Omega \cdot \nabla(\cdot) + \sigma_T(\cdot), \\ \mathcal{S}(\cdot) &\equiv \frac{\sigma_S}{4\pi} \int_{\mathbb{S}^2} (\cdot) \, \mathrm{d}\Omega'. \end{aligned} \tag{1.9}$$

Using these operators, (1.6) can be written as

$$\mathcal{T}\psi(\mathbf{r},\Omega) = \mathcal{S}\psi(\mathbf{r},\Omega) + Q(\mathbf{r}). \tag{1.10}$$

The third operator is just a further simplification of the scatter operator, and is defined to be

$$\mathcal{P}(\cdot) \equiv \frac{1}{4\pi} \int_{\mathbb{S}^2} (\cdot) \, \mathrm{d}\Omega'. \tag{1.11}$$

This allows us to define the scatter operator as $\mathcal{S} \equiv \sigma_S \mathcal{P}$, and will prove useful in our later analysis.

1.2 The Neutron Transport Equation in 1D

Much of our later analysis will be presented in one dimension only, and we will now reduce the simplified 3D version of the transport equation, (1.6), to one dimension. By 'one dimension', we mean one spatial dimension; we will also include one angular dimension. Overall, the total dimension of the equation of interest will reduce from five dimensions (in (1.6)) to two dimensions. While this is less physically relevant, we hope to extend theory we develop back to three spatial dimensions when possible. We will be working in what is known as *slab geometry*, and must adjust our angular and spatial domains accordingly. Firstly, our spatial variable, $\mathbf{r}$, will become $x \in [a,b] \subset \mathbb{R}$. Also, considering standard polar coordinates on $\mathbb{S}^2$, we denote by μ the contribution of Ω in the spatial z-direction (see figure 1-1) [7]. Then μ parametrises the unit 'sphere'

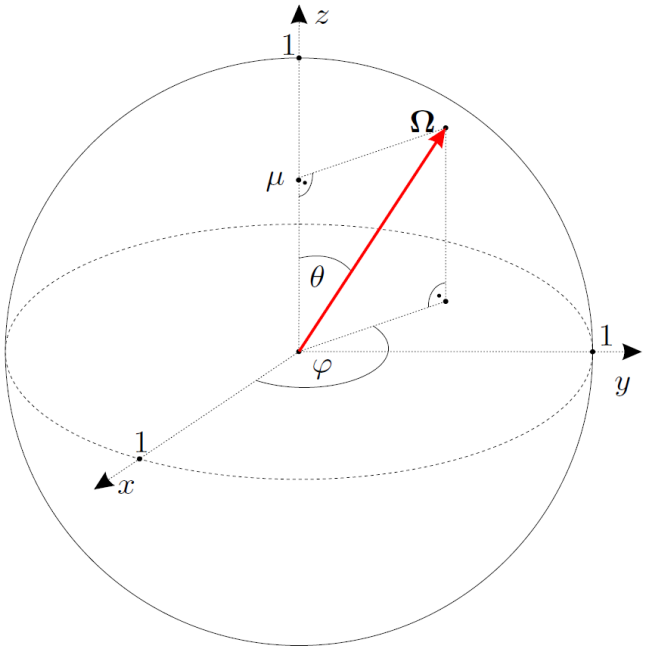

Figure 1-1: *Standard polar coordinates on $\mathbb{S}^2$, showing the contribution of Ω in the z-direction. Taken from [27].*

in 1D via $\mu = \cos(\theta)$ for $\theta \in [0, \pi]$, so $\mu \in [-1, 1]$.

Under these assumptions, the transport equation (1.6) becomes

$$\mu \frac{\partial}{\partial x}\psi(x,\mu) + \sigma_T \psi(x,\mu) = \frac{\sigma_S}{2}\int_{-1}^{1} \psi(x,\mu)\, \mathrm{d}\mu + Q(x). \tag{1.12}$$

The factor of $\frac{1}{2}$ arises after integrating over the azimuthal angle, see [23] Section 3.2. We will refer to (1.12) whenever we are looking at theory in one dimension.

1.2.1 Boundary Conditions

As in the 3D case, (1.12) can only be solved when combined with some relevant boundary conditions. We will consider the same two types of condition for the 1D case as in the 3D case: *vacuum* boundary conditions and *reflecting* boundary conditions.

First of all, the 1D version of vacuum boundary conditions are specified as follows.

$$\begin{aligned} \psi(a,\mu) &= 0 \quad \text{for } \mu > 0, \\ \psi(b,\mu) &= 0 \quad \text{for } \mu < 0. \end{aligned} \tag{1.13}$$

So we have that at the left-most end of the domain ($x = a$), the flux in the inward direction (positive μ) is zero, and at the right-most end of the domain ($x = b$), the flux in the inward direction (negative μ) is zero.

Next, reflecting boundary conditions in 1D are defined as follows.

$$\begin{aligned} \psi(a,-\mu) &= \psi(a,\mu), \\ \psi(b,-\mu) &= \psi(b,\mu). \end{aligned} \tag{1.14}$$

This ensures that outgoing flux at each end of the domain equals the opposing incoming flux. This effectively prevents neutrons from escaping the system, causing them to instead 'reflect' back inside.

As mentioned in Section 1.1.2 we will only consider solving (1.12) with vacuum boundary conditions specified by (1.13). We will again define the space we are working within to be

$$L^2\left([a,b],L^1[-1,1]\right) \equiv \left\{ \psi : [a,b]\times[-1,1]\to\mathbb{R} \ : \ \int_{[a,b]} \|\psi(x,\cdot)\|^2_{L^1[-1,1]} \ \mathrm{d}x < \infty \right\},$$

where

$$\|\psi\|^2_{L^2([a,b],L^1[-1,1])} = \int_{[a,b]} \|\psi(x,\cdot)\|^2_{L^1[-1,1]} \ \mathrm{d}x,$$

and

$$\|\psi(x,\cdot)\|_{L^1[-1,1]} \equiv \int_{[-1,1]} |\psi(x,\mu)| \ \mathrm{d}\mu,$$

is the usual L^1-norm. With this we can say that in solving (1.12), we are looking for some $\psi \in L^2\left([a,b],L^1[-1,1]\right)$ that satisfies vacuum boundary conditions, (1.13), with $\frac{\partial}{\partial x}\psi \in L^2\left([a,b],L^1[-1,1]\right)$ also.

1.2.2 Operator Form

For the 1D case we can introduce the same three operators as before ($\mathcal{T}$, $\mathcal{S}$ and $\mathcal{P}$) but now they are defined as follows

$$\begin{aligned} \mathcal{T}(\cdot) &\equiv \mu\frac{\partial}{\partial x}(\cdot) + \sigma_T(\cdot), \\ \mathcal{S}(\cdot) &\equiv \frac{\sigma_S}{2}\int_{[-1,1]}(\cdot)\ \mathrm{d}\mu. \\ \mathcal{P}(\cdot) &\equiv \ \frac{1}{2}\int_{[-1,1]}(\cdot)\ \mathrm{d}\mu. \end{aligned} \tag{1.15}$$

Again the $\mathcal{T}$ and $\mathcal{S}$ operators just define the transport and scatter parts of the transport equation as in 3D, and $\mathcal{P}$ is just an integral operator over angle. Using these, (1.12) can be written as

$$\begin{aligned} \mathcal{T}\psi(x,\mu) = &\quad \mathcal{S}\psi(x,\mu) + Q(x). \\ &\equiv \sigma_S\mathcal{P}\psi(x,\mu) + Q(x). \end{aligned} \tag{1.16}$$

During our later analysis, it should be clear from the context whether we are refering to the 3D versions ((1.9) and (1.11)) or to these 1D versions of the operators. For this reason we will not use a notational difference to distinguish them.

1.3 Solution Methods

In this section we will talk about some of the different types of methods that are used to solve the transport equation in modelling nuclear fission reactors. Broadly these methods can be broken down into two genres: *deterministic* methods and *Monte Carlo* (stochastic) methods. Monte Carlo methods are discussed widely in the literature (see [20] Chapter 7, [10] Chapter 9) and are currently used to model reactor criticality. These methods have an advantage in that they do not depend upon meshing the domain, and so the complexity of the domain does not dramatically affect the solve time. For this reason they are often preferred for modelling complex geometrical set-ups. The majority of our analysis will be focussed around deterministic methods.

Deterministic methods are those that will always produce the same output for a given input. These methods discretise the transport equation and form a system of coupled algebraic equations which can then be solved. This can involve using iterative methods (provided they don't contain calls to random variables), such as *Krylov* methods (see [14], [25], [26]) that are to be one of the focus points of our research (see Section 1.4). Deterministic approaches include methods like *discrete ordinates* (the S_N-method), *spherical harmonics* (the P_N-method) and *diffusion approximation*.

1.3.1 Discrete Ordinates

The *discrete ordinates* method works by sampling the angular variable at a number of discrete points, and then replacing the integrals over angle in (1.2) (or (1.12)) by weighted quadrature summations. The quadrature points and weights should be chosen so that all directions of the neutron flux are given equal importance. This yields a semidiscrete system of equations, which can then be discretised in space via some finite difference or finite element method, allowing a numerical solution method to be applied. This method is often called the S_N-method, and further information on it can be found in [29] Chapter 4, [20] Chapters 3 and 4, [28] Chapter 9, and [12] Chapter 9 among others.

1.3.2 Spherical Harmonics

The *spherical harmonics* method for solving the neutron transport equation works by expanding the angular component of the neutron flux in terms of spherical harmonics. By truncating this expansion a finite system of semidiscrete equations can be obtained. This can be further simplified using orthogonality. Discretising the spatial variable

using finite difference methods or finite element methods once again allows for the application of a suitable solver. This method is often called the P_N-method, and further information can be found in [5] Chapter 3 or [20] Chapter 3.

1.3.3 Diffusion Approximation

The fundamental idea behind this solution method is that, under certain conditions, a quantity known as the *scalar flux* can be approximated well by the solution to a specific diffusion equation. The *scalar flux*, denoted ϕ, is defined to be

$$\phi(\mathbf{r}) \equiv \mathcal{P}\psi(\mathbf{r}, \Omega), \tag{1.17}$$

where $\mathcal{P}$ is defined in (1.11), and the corresponding diffusion equation is given by

$$-\frac{1}{3\hat{\sigma}_T}\nabla \cdot \nabla\phi(\mathbf{r}) + \hat{\sigma}_A\phi(\mathbf{r}) = Q(\mathbf{r}). \tag{1.18}$$

The $\hat{\cdot}$ notation on the cross-sections is used here to indicate nondimensionality, and will be more thoroughly explained in Section 3.2.

To make this approximation several assumptions, given in (for example) [19], are made. We will state these and understand their consequences in Chapter 3. Unfortunately one of the assumptions does not hold near domain boundaries, but the approximation can actually still give accurate predictions by working on a homogenised domain where the cross-sections are averaged spatially (see [28] Chapter 3, p.47).

Extension of this theory into an iterative acceleration scheme, known as *diffusion synthetic acceleration*, or DSA, will also be addressed in Chapter 3. Good information on DSA can be found in [2] Chapters 1 and 2, and we will reference other relevant papers in Chapter 3. Work on this solution method has formed a central part of our focus so far, and will hopefully form part of an eventual thesis.

1.4 Research Aims and Future Work

In this section we will state and then justify the current aims of our research, and then later talk about what we are doing to achieve these. The current aims are:

1. To investigate Krylov methods for use in solving the neutron transport equation.
2. To investigate diffusion acceleration and understand its benefits and limitations, with the eventual aim of forming it as a preconditioner.
3. To combine aims 1 and 2, and look at applying acceleration and preconditioning methods to speed up Krylov solves of the neutron transport equation.

Iterative solves are used in current industrial deterministic software for solving criticality problems including the neutron transport problem. One example is in the WIMS code (part of the ANSWERS® Software Service provided by AMEC) where two of the deterministic methods mentioned in section 1.3 can be used (S_N and diffusion theory) as well as the method of characteristics and the method of *collision probabilities* (more information on both of these methods within a nuclear physics setting can be found in [8] and [28]), alongside iterative solvers. They are still a very relevant part of the industry and as such any improvements in efficiency (and so accuracy) of solves can only be beneficial for both energy and environmental concerns alike. Firstly for reducing associated risks, and secondly for continuing to satisfy growing energy demands [28](Preface). Krylov methods are well understood mathematically (see [25] and [26]) and make good intuitive sense (see [14]). Currently most industrial level nuclear modelling software packages use a simple iterative method called *source iteration* to some extent, which we will introduce in Chapter 2. Information on source iteration can be found in [7], [12], [27], and many others. Various methods of acceleration, including Krylov methods, are utilised to speed up convergence, and so work in this area is still very relevant.

In this report we focus primarily on the second aim. *Preconditioning* a system involves transforming it (via some process or operator known as a *preconditioner*) into a form more easily solved using iterative methods. The key to this is that the cost of preconditioning should not outweigh the benefits. Preconditioning is a frequently used process, backed up with a wealth of mathematical knowledge and understanding (see [12] and [25], or [2] for a transport specific text). In particular the case of preconditioning Krylov subspace methods has been considered in detail in [26] Chapter 9 and in [6].

In the neutron transport literature it is accepted that the diffusion equation can be a good approximation of the neutron transport equation under some circumstances (see in particular [28] Chapter 3, [2], [5], [29], [19] and good boundary condition discussion can be found in [13], with the discrete case looked at in [15], [16] and [11]). We will use an asymptotic argument to obtain an approximate diffusion form of the transport equation in Chapter 3, and will look at relevant boundary conditions. This diffusion approximation can be used to construct an acceleration scheme known as *diffusion synthetic acceleration*, which works in conjunction with another iterative scheme (such as source iteration) and uses diffusion solves to update the approximate solution at each iteration. See [2] Chapters 2 and 3, and [4] for analysis; see [3] and [17] for application. Acceleration schemes can be shown to be equivalent to preconditioning methods ([12] and [2] Chapter 1 for discussion) and we are hoping to formulate diffusion synthetic acceleration as a preconditioner to a Krylov solver. If we are successful, this would allow us to utilise the existing vast knowledge about preconditioning Krylov methods

mentioned earlier.

We have made steps in this direction by understanding how a block operator form of the transport equation relates to the diffusion equation (see Chapter 4). We have made efforts to understand the error incurred by the diffusion equation in this form (see Theorems 4.4 and 4.6) and in Chapter 5 we look at how this influences the implementation of the method.

A lot of effort has been put into overcoming numerical instability issues caused by certain discretisations of the transport and diffusion equations (see [3] for the recognised solution, [17] for some follow up work), and this has led to a good understanding of how to guarantee stability in diffusion synthetic acceleration schemes, which will be introduced in Section 3.3. However there have been fewer thorough attempts to analyse the scheme mathematically with the aim of fully understanding what causes errors and justifying methods of minimising them (one discussion is in [4]. This paper looks very relevant though I do not understand it to any depth yet).

There is an understanding that transport theory transitions into diffusion theory as the scattering cross-section converges to the total cross-section (see [19], and in particular [11]). This can be shown by obtaining the diffusion equation from the transport equation using an asymptotic argument given in [13], [18] and [19]. We will give an asymptotic derivation of the continuous diffusion approximation in Chapter 3 and attempt to demonstrate this transition in Chapter 6.

In the coming months we have several objectives. We hope to start looking at higher dimensional problems, starting with writing a code to solve a 2D version of the transport equation. Discussions during a recent visit to AMEC have resulted in two model 2D problems which could be considered, and benchmark solutions to these problems can be obtained from researchers at the University of Imperial.

As will be noted in Chapter 6 we would like to start writing programs in a language that allows for arbitrary numerical precision. This should help us overcome an issue highlighted in Sections 6.3 and 6.4.

On the theoretical side we aim to complete the proof of Theorem 4.6, either by proving the assumption made or by a different method. We also plan to reduce the number of assumptions made in Theorem 4.4. In the discrete case, we would like to prove the symmetry of the Schur matrix $I - PT^{-1}\Sigma$ defined in Chapter 5, as well as prove results about its maximum and minimum eigenvalues. Both of these have been observed numerically.

Lastly we would like to start understanding how diffusion synthetic acceleration (see Section 3.3) can be implemented as a preconditioner. Some effort in this direction has been made, however we would like to go a lot further. Some material that should help with this is known about (eg. [4], [30]).

Chapter 2

Source Iteration

2.1 Introduction

In this chapter we will look at a basic iterative method known as *source iteration*. In Section 2.2 we will give a statement of the source iteration algorithm, and will go on to prove some results about its convergence. These will highlight a specific situation in which source iteration has the potential to converge very slowly. In Section 2.3 we will present a method which, when combined with work in Chapter 3, will overcome this limitation.

2.2 Source Iteration in 3D

In this section we will first have a look at a possible iterative method for solving (1.10), and then we will use results from F. Scheben, 2011, [27] to understand what influences the convergence of the method.

One possible basic iterative method for solving the neutron transport equation is known as *source iteration*. Using the definition of the *scalar flux* given by (1.17) we can write the 3D transport equation, (1.10), as

$$\mathcal{T}\psi(\mathbf{r},\Omega) = \sigma_S\phi(\mathbf{r}) + Q(\mathbf{r}) \tag{2.1}$$

with boundary conditions (1.7). From here source iteration can be defined easily as

follows

Algorithm 1: Source iteration (3D)

1. Start with some initial $\phi^{(0)}(\mathbf{r})$,
2. solve
$$\mathcal{T}\psi^{(i+1)}(\mathbf{r},\Omega) = \sigma_S\phi^{(i)}(\mathbf{r}) + Q(\mathbf{r}), \tag{2.2}$$
for $\psi^{(i+1)}(\mathbf{r},\Omega)$, where $\psi^{(i+1)}$ satisfies vacuum boundary conditions (1.7),
3. integrate to find $\phi^{(i+1)}(\mathbf{r}) = \mathcal{P}\psi^{(i+1)}(\mathbf{r},\Omega)$, and return to step 2.

2.2.1 Convergence of Source Iteration in 3D

A natural question is: under what conditions does Algorithm 1 converge? To answer this we will look at two results from F. Scheben, 2011, [27] (Lemma 2.3 and Theorem 2.9 respectively).

First however, let us define the inverse operator, $\mathcal{T}^{-1} : L^2(V) \to L^2(V, L^1(\mathbb{S}^2))$, to be the inverse of the operator $\mathcal{T}$ defined in (1.9) with vacuum boundary conditions, i.e. $f(\mathbf{r},\Omega) \equiv \mathcal{T}^{-1}g(\mathbf{r})$ satisfies

$$\mathcal{T}f(\mathbf{r},\Omega) = g(\mathbf{r}),$$

and also the vacuum conditions (1.7). The two results from [27] can now be given.

Lemma 2.1:
If $\psi(\mathbf{r},\Omega) \in L^2\left(V, L^1(\mathbb{S}^2)\right)$ *satisfies*

$$\mathcal{T}\psi(\mathbf{r},\Omega) = g(\mathbf{r}), \tag{2.3}$$

where $g \in L^2(V)$*, then*

$$\phi(\mathbf{r}) = \left(\mathcal{K}_{\sigma_T}g\right)(\mathbf{r}) \equiv \left(\mathcal{P}\mathcal{T}^{-1}g\right)(\mathbf{r}), \tag{2.4}$$

where $\mathcal{K}_{\sigma_T}$ *is defined in [27] (equation (2.11)).*

Theorem 2.2:

If $\mathcal{K}_{\sigma_T}$ is the operator used in Lemma 2.1 then

$$\|\mathcal{K}_{\sigma_T}\|_{\mathscr{L}(L^2(V))} \leq \frac{1}{\sigma_T}, \tag{2.5}$$

where $\mathscr{L}(L^2(V))$ denotes the space of linear operators mapping from $L^2(V)$ to $L^2(V)$.

Here, $\|\cdot\|_{\mathscr{L}(L^2(V))}$ is the standard operator norm defined as

$$\|\mathcal{K}_{\sigma_T}\|_{\mathscr{L}(L^2(V))} \equiv \sup\left\{ \frac{\|\mathcal{K}_{\sigma_T} g\|_{L^2(V)}}{\|g\|_{L^2(V)}} \ : \ g \in L^2(V), g \neq 0 \right\} \tag{2.6}$$

Using these two results, we can now state and prove the following Lemma which we will then use to bound the error incurred at each step of source iteration.

Lemma 2.3:
If $\mathcal{K}_{\sigma_T}$ is the operator used in Lemma 2.1 and $\psi(\mathbf{r},\Omega) \in L^2\left(V, L^1(\mathbb{S}^2)\right)$ satisfies

$$\mathcal{T}\psi(\mathbf{r},\Omega) = g(\mathbf{r}), \quad g \in L^2(V),$$

then

$$\|\phi\|_{L^2(V)} \leq \frac{1}{\sigma_T} \|g\|_{L^2(V)}, \tag{2.7}$$

where $\phi(\mathbf{r}) = \mathcal{P}\psi(\mathbf{r},\Omega)$.

Proof.
The operator norm definition (2.6) gives

$$\frac{\|\mathcal{K}_{\sigma_T} g\|_{L^2(V)}}{\|g\|_{L^2(V)}} \leq \|\mathcal{K}_{\sigma_T}\|_{\mathscr{L}(L^2(V))} \leq \frac{1}{\sigma_T}. \tag{2.8}$$

Since $\psi(\mathbf{r},\Omega) \in L^2\left(V, L^1(\mathbb{S}^2)\right)$ satisfies (2.3), we know from Lemma 2.1 that $\phi(\mathbf{r}) = \left(\mathcal{K}_{\sigma_T} g\right)(\mathbf{r})$. Thus we have

$$\frac{\|\phi\|_{L^2(V)}}{\|g\|_{L^2(V)}} \leq \frac{1}{\sigma_T}. \tag{2.9}$$

Multiplying through by $\|g\|_{L^2(V)}$ yields the result. □

Next, subtracting (2.2) from (1.10) leaves

$$\mathcal{T}e^{(i+1)}(\mathbf{r},\Omega) = \sigma_T E^{(i)}(\mathbf{r}), \tag{2.10}$$

where

$$\begin{aligned} e^{(i)}(\mathbf{r},\Omega) &\equiv \left(\psi - \psi^{(i)}\right)(\mathbf{r},\Omega), \\ E^{(i)}(\mathbf{r}) &\equiv \left(\phi - \phi^{(i)}\right)(\mathbf{r}), \end{aligned} \tag{2.11}$$

with $E^{(i)}(\mathbf{r}) = \mathcal{P}e^{(i)}(\mathbf{r},\Omega)$ as you would expect. We can now prove the following convergence result.

Lemma 2.4:
Under the definitions in (2.11)*, the following bound holds*

$$\left\|E^{(i+1)}\right\|_{L^2(V)} \leq \frac{\sigma_S}{\sigma_T}\left\|E^{(i)}\right\|_{L^2(V)}. \tag{2.12}$$

Proof.
Combining (2.10) with Lemma 2.3 we immediately obtain

$$\left\|E^{(i+1)}\right\|_{L^2(V)} \leq \frac{1}{\sigma_T}\left\|\sigma_S E^{(i)}\right\|_{L^2(V)} \leq \frac{\sigma_S}{\sigma_T}\left\|E^{(i)}\right\|_{L^2(V)}. \tag{2.13}$$

□

Since $\sigma_S < \sigma_T$, Lemma 2.4 implies that source iteration converges for any starting guess. However, this convergence may be slow if σ_S/σ_T is close to one. An equivalent result to Lemma 2.4 can be found for the one dimensional case, and shows that 1D source iteration suffers the same convergence bound as the 3D case. Details are given in the Appendix, Section A.1 for completeness. In Chapter 3 we will introduce a regime in which σ_S/σ_T is close to one, but first we will suggest a different iterative method that builds upon source iteration.

2.3 Improving upon Source Iteration

We have seen (in Lemma 2.4) that source iteration converges quite robustly, but has the potential for slow convergence if σ_S/σ_T is close to one.

In this section we will introduce an iterative 'framework', with the motivation being to create a method which maintains source iteration's basic convergence, but will also converge quickly in situations where source iteration would converge slowly. The idea is to add an update step into standard source iteration, though we will not explain how the update can be found.

The framework is given in the following algorithm.

Algorithm 2: Updated source iteration (3D)

1. Start with some initial $\phi^{(0)}(\mathbf{r})$,
2. solve
$$\mathcal{T}\psi^{(i+1/2)}(\mathbf{r},\Omega) = \sigma_S\phi^{(i)}(\mathbf{r}) + Q(\mathbf{r}), \tag{2.14}$$
for $\psi^{(i+1/2)}(\mathbf{r},\Omega)$,
3. integrate to find $\phi^{(i+1/2)}(\mathbf{r}) = \mathcal{P}\psi^{(i+1/2)}(\mathbf{r},\Omega)$,
4. update via $\phi^{(i+1)}(\mathbf{r}) = \phi^{(i+1/2)}(\mathbf{r}) + \delta^{(i+1/2)}(\mathbf{r})$, and return to step 2.

We want to choose the update so that

$$\delta^{(i+1/2)}(\mathbf{r}) \approx \phi(\mathbf{r}) - \phi^{(i+1/2)}(\mathbf{r}),$$

balancing the accuracy of the approximation against its ease of calculation. The aim is to minimise $\left\|E^{(i+1)}\right\|_{L^2(V)}$, and ideally whatever method is used to choose the update should be most accurate when σ_S is close to σ_T. This would hopefully offset the weak convergence of source iteration in that situation. In Section 3.3 we will see that the diffusion equation (1.18) can be used to find the update.

Chapter 3

Diffusion Approximation

3.1 Introduction

In Section 2.2 we saw that source iteration has the potential to converge very slowly if σ_S/σ_T is close to 1. In Section 3.2 we will see how the specific diffusion equation given in (1.18) can be used to approximate the solution to the transport equation in precisely the case when $\sigma_S/\sigma_T \approx 1$. We will show that this diffusion equation can be obtained by working from a dimensional version of the transport equation (given by (3.1)) and using an asymptotic argument. To achieve this we will need to introduce and understand what is meant by a *diffusive regime*. A discussion of the diffusion boundary conditions will follow where it will be seen why these pose a problem. Lastly it will be mentioned that this approximation can be used to find an update, δ, to be used by Algorithm 2.

3.2 The Diffusion Approximation in 3D

3.2.1 Asymptotic Transport Equation

In this section we will obtain a version of the transport equation in terms of a small parameter, ϵ, which will be defined. This version will allow us to conduct an asymptotic argument to obtain the diffusion equation given by (1.18). We will use a method given in [13] and [19].

To begin with we will state the neutron transport equation in dimensional form.

$$\Omega \cdot \tilde{\nabla}\tilde{\psi}(\tilde{\mathbf{r}}, \Omega) + \sigma_T \tilde{\psi}(\tilde{\mathbf{r}}, \Omega) = \frac{\sigma_S}{4\pi} \int_{\mathbb{S}^2} \tilde{\psi}(\tilde{\mathbf{r}}, \Omega)\, \mathrm{d}\Omega + \tilde{Q}(\tilde{\mathbf{r}}), \tag{3.1}$$

where the $\tilde{}$ notation denotes a dimensional quantity, and $\tilde{\mathbf{r}} \in \tilde{V} \subset \mathbb{R}^3$ is the dimensionless spatial variable. At this point we introduce a distance called a *scale length*, denoted ρ, which is defined in [19], p.288 to be the distance over which the neutron flux

and non-fission source vary by "at most an $O(1)$ amount". The discussions of choosing such a distance given in [19] is heuristic. Despite not having a well defined procedure it is assumed that such a distance can be chosen, with certain specific examples given. For our purposes we will proceed under the assumption that for our problem such a distance can be chosen. Using this we can introduce a dimensionless version of the spatial variable,

$$\mathbf{r} \equiv \frac{\tilde{\mathbf{r}}}{\rho}. \tag{3.2}$$

From here we define the dimensionless neutron flux counterpart as $\psi(\mathbf{r}, \Omega) \equiv \tilde{\psi}(\tilde{\mathbf{r}}, \Omega)$ and also obtain $\tilde{\nabla} = \frac{1}{\rho}\nabla$. Using these, (3.1) becomes

$$\Omega \cdot \nabla\psi(\mathbf{r}, \Omega) + \rho\sigma_T\psi(\mathbf{r}, \Omega) = \frac{\rho\sigma_S}{4\pi}\int_{\mathbb{S}^2} \psi(\mathbf{r}, \Omega)\, \mathrm{d}\Omega + \rho\tilde{Q}(\rho\mathbf{r}). \tag{3.3}$$

Another length we need to understand is called a *mean-free path*, and is the typical distance a neutron travels between successive collisions. It is equal to the reciprocal of the average total cross-section, which is typically denoted $\langle\sigma_T\rangle^{-1}$. Using this length we now define

$$\epsilon \equiv \frac{\langle\sigma_T\rangle^{-1}}{\rho} = \frac{\text{typical mean free path}}{\text{scale length}}. \tag{3.4}$$

If we were working with spatially dependent cross-sections, we would now non-dimensionalise by saying

$$\hat{\sigma}_T = \frac{\sigma_T}{\langle\sigma_T\rangle}, \tag{3.5}$$

and then note that this yields

$$\rho\sigma_T = \frac{\hat{\sigma}_T}{\epsilon}. \tag{3.6}$$

However, in a homogeneous domain with constant cross-sections, $\langle\sigma_T\rangle \equiv \sigma_T$, thus $\hat{\sigma}_T = 1$. During this report we will retain this $\hat{\sigma}_T$ notation (and equivalents for the absorption and scattering cross-sections) to 'keep track' of their influence on our analysis. This will help us understand how our work is applicable to cases with piecewise constant or fully spatially dependent cross-sections.

At this point, we shall assume that the problem we are working of is *diffusive*. This is defined concisely in [19], p.284, to be a regime that satisfies the following three assumptions:

1. The physical medium is several mean free paths thick. This is often referred to as being *optically thick*.

2. Neutron collisions are scattering-dominated, i.e. $\sigma_A \ll \sigma_S$.

3. The neutron flux, cross-sections and source are continuous, and vary by only a small amount in space over the distance of a mean free path.

To clarify, by "a small amount" we mean an amount significantly smaller than the amount they vary over the distance of a scale length, ρ. Thus assumption 3 can be satisfied by requiring there to be many mean-free paths in a scale length, and so

$$\epsilon \ll 1. \tag{3.7}$$

We can now further say that in order for the medium to be optically thick, it must be about as big (or bigger) than a scale length. This just leaves assumption 2, which requires that σ_A be small in relation to σ_S, and thus that σ_S/σ_T be close to 1. To enforce this we set the condition that

$$\rho\sigma_A = \epsilon\hat{\sigma}_A \ll 1. \tag{3.8}$$

We impose a similar scaling to the dimensional source term, and define

$$\rho\tilde{Q}(\rho\mathbf{r}) = \epsilon Q(\mathbf{r}). \tag{3.9}$$

This particular scaling of the non-fission source term ensures that an $O(1)$ change in the solution, ψ, corresponds to an $O(1)$ change in Q. Combining all of the above, and noting that $\rho\sigma_S = \rho\sigma_T - \rho\sigma_A$, results in a fully non-dimensional version of the transport equation given by

$$\Omega \cdot \nabla\psi(\mathbf{r},\Omega) + \frac{\hat{\sigma}_T}{\epsilon}\psi(\mathbf{r},\Omega) = \frac{1}{4\pi}\left[\frac{\hat{\sigma}_T}{\epsilon} - \hat{\sigma}_A\epsilon\right]\int_{\mathbb{S}^2}\psi(\mathbf{r},\Omega)\,\mathrm{d}\Omega + \epsilon Q(\mathbf{r}). \tag{3.10}$$

This form of the transport equation is parametrised by ϵ, with the property that taking ϵ smaller moves you further into a diffusive regime. Also notice that

$$\begin{aligned}\frac{\sigma_S}{\sigma_T} &= \frac{\epsilon}{\hat{\sigma}_T}\left[\frac{\hat{\sigma}_T}{\epsilon} - \hat{\sigma}_A\epsilon\right] \\ &= \left[1 - \epsilon^2\frac{\hat{\sigma}_A}{\hat{\sigma}_T}\right]\end{aligned}$$

This is the quantity that governs the estimate of convergence of source iteration, as seen in Lemma 2.4, Section 2.2. Therefore taking $\epsilon \to 0$ causes the estimate of convergence of source iteration to deteriorate with ϵ^2. Thus we conclude: within a diffusive regime, source iteration has the potential to perform poorly.

It was to overcome situations such as this that we defined Algorithm 2, but we still need to determine how the update, δ, is to be specified. In the remainder of this section

we will show how a diffusion approximation can be derived that well approximates the solution to the neutron transport equation within a diffusive regime. Ultimately, it will be this equation that is used to determine a relevant update, δ.

3.2.2 Deriving the Diffusion Equation

In this section we will use the specific version of the transport equation, (3.10), derived above to obtain the diffusion equation given by (1.18) via an asymptotic argument.

Firstly, following E. Larsen, J. E. Morel and W. F. Miller, Jr. [19], we introduce the following asymptotic expansion of the neutron flux in terms of the variable ϵ

$$\psi(\mathbf{r},\Omega) \sim \sum_{k=0}^{\infty} \epsilon^k \psi^{(k)}(\mathbf{r},\Omega). \tag{3.11}$$

Substituting this into (3.10) (and dropping the dependencies for clarity) leaves

$$\sum_{k=0}^{\infty} \left(\epsilon^k \Omega \cdot \nabla \psi^{(k)} + \hat{\sigma}_T \epsilon^{k-1} \psi^{(k)} \right) = \frac{1}{4\pi} \left[\frac{\hat{\sigma}_T}{\epsilon} - \epsilon \hat{\sigma}_A \right] \int_{\mathbb{S}^2} \sum_{k=0}^{\infty} \epsilon^k \psi^{(k)} \, \mathrm{d}\Omega + \epsilon Q, \tag{3.12}$$

and the coefficients of the first three powers of ϵ in (3.12) are

$$\begin{aligned}
\epsilon^{-1} : \quad & \hat{\sigma}_T \psi^{(0)} = \frac{\hat{\sigma}_T}{4\pi} \int_{\mathbb{S}^2} \psi^{(0)} \, \mathrm{d}\Omega, \\
\epsilon^{0} \quad : \quad & \Omega \cdot \nabla \psi^{(0)} + \hat{\sigma}_T \psi^{(1)} = \frac{\hat{\sigma}_T}{4\pi} \int_{\mathbb{S}^2} \psi^{(1)} \, \mathrm{d}\Omega, \\
\epsilon^{1} \quad : \quad & \Omega \cdot \nabla \psi^{(1)} + \hat{\sigma}_T \psi^{(2)} = \frac{\hat{\sigma}_T}{4\pi} \int_{\mathbb{S}^2} \psi^{(2)} \, \mathrm{d}\Omega - \frac{\hat{\sigma}_A}{4\pi} \int_{\mathbb{S}^2} \psi^{(0)} \, \mathrm{d}\Omega + Q.
\end{aligned} \tag{3.13}$$

If we define

$$\phi^{(k)}(\mathbf{r}) \equiv \frac{1}{4\pi} \int_{\mathbb{S}^2} \psi^{(k)}(\mathbf{r},\Omega) \, \mathrm{d}\Omega, \tag{3.14}$$

then the coefficient of ϵ^{-1} gives us that

$$\psi^{(0)}(\mathbf{r},\Omega) = \phi^{(0)}(\mathbf{r}). \tag{3.15}$$

We will refer back to this equation later in this section. Combining this with the coefficient of ϵ^0 we get

$$\Omega \cdot \nabla \phi^{(0)}(\mathbf{r}) + \hat{\sigma}_T \psi^{(1)}(\mathbf{r},\Omega) = \hat{\sigma}_T \phi^{(1)}(\mathbf{r}). \tag{3.16}$$

Now combining (3.15) and (3.16) with the coefficient of ϵ^1 leaves

$$\Omega \cdot \nabla \left(\phi^{(1)}(\mathbf{r}) - \frac{1}{\hat{\sigma}_T} \Omega \cdot \nabla \phi^{(0)}(\mathbf{r}) \right) + \hat{\sigma}_T \left(\psi^{(2)}(\mathbf{r}, \Omega) - \phi^{(2)}(\mathbf{r}) \right) = Q(\mathbf{r}) - \hat{\sigma}_A \phi^{(0)}(\mathbf{r}).$$

If we now integrate both sides over angle, Ω, and scale by $1/4\pi$ we get

$$\begin{aligned} \frac{1}{4\pi} \int_{\mathbb{S}^2} \Omega \cdot \nabla \phi^{(1)} \, \mathrm{d}\Omega - \frac{1}{4\pi \hat{\sigma}_T} \int_{\mathbb{S}^2} \Omega \cdot \nabla (\Omega \cdot \nabla \phi^{(0)}) \, \mathrm{d}\Omega \\ + \hat{\sigma}_T \left(\frac{1}{4\pi} \int_{\mathbb{S}^2} \psi^{(2)} \, \mathrm{d}\Omega - \frac{\phi^{(2)}}{4\pi} \int_{\mathbb{S}^2} \, \mathrm{d}\Omega \right) + \hat{\sigma}_A \phi^{(0)} = Q. \end{aligned} \tag{3.17}$$

Since $\int_{\mathbb{S}^2} \mathrm{d}\Omega = 4\pi$, we know that

$$\frac{1}{4\pi} \int_{\mathbb{S}^2} \psi^{(2)} \, \mathrm{d}\Omega - \frac{\phi^{(2)}}{4\pi} \int_{\mathbb{S}^2} \, \mathrm{d}\Omega = 0. \tag{3.18}$$

It also holds that

$$\begin{aligned} \frac{1}{4\pi} \int_{\mathbb{S}^2} \Omega \cdot \nabla \phi^{(1)} \, \mathrm{d}\Omega = 0, \\ \frac{1}{4\pi \hat{\sigma}_T} \int_{\mathbb{S}^2} \Omega \cdot \nabla (\Omega \cdot \nabla \phi^{(0)}) \, \mathrm{d}\Omega = \frac{1}{3\hat{\sigma}_T} \nabla \cdot \nabla \phi^{(0)}. \end{aligned} \tag{3.19}$$

These equalities are consequences of Lemmas A.5 and A.6 given in the Appendix, Section A.2. Combining (3.18) and (3.19) with (3.17) we finally obtain

$$-\frac{1}{3\hat{\sigma}_T} \nabla \cdot \nabla \phi^{(0)}(\mathbf{r}) + \hat{\sigma}_A \phi^{(0)}(\mathbf{r}) = Q(\mathbf{r}). \tag{3.20}$$

This is the diffusion equation that was introduced earlier, (1.18), and is called the *3D diffusion equation*. It can be found in [21], equation (2-21), for the multi-group case with inhomogeneous scattering.

From (3.11) and (3.15) we know that

$$\begin{aligned} \psi(\mathbf{r}, \Omega) &= \psi^{(0)}(\mathbf{r}) + O(\epsilon), \\ &= \phi^{(0)}(\mathbf{r}) + O(\epsilon), \\ &\approx \phi^{(0)}(\mathbf{r}). \end{aligned} \tag{3.21}$$

Therefore, when ϵ is small, we can use the 3D diffusion equation to approximate the neutron flux. This fact forms the core of an acceleration scheme which will be the focus of Section 3.3.

In our later analysis, we will be working in 1D and so will include here a statement of the 1D diffusion equation

$$\frac{-1}{3\hat{\sigma}_T}\frac{\mathrm{d}^2}{\mathrm{d}x^2}\phi(x) + \hat{\sigma}_A\phi(x) = Q(x). \tag{3.22}$$

This can be obtained using an identical argument to the one just presented, and can be used to approximate the scalar flux,

$$\phi(x) \equiv \int_{[-1,1]} \psi(x,\mu)\,\mathrm{d}\mu,$$

where $\psi(x,\mu)$ satisfies the non-dimensional 1D transport equation,

$$\mu\frac{\partial}{\partial x}\psi(x,\mu) + \frac{\hat{\sigma}_T}{\epsilon}\psi(x,\mu) = \left[\frac{\hat{\sigma}_T}{\epsilon} - \epsilon\hat{\sigma}_A\right]\phi(x) + \epsilon Q(x), \tag{3.23}$$

with vacuum boundary conditions given by (1.13).

3.2.3 Boundary Conditions

Finding suitable boundary conditions associated with the diffusion equation, (3.20), is a non-trivial problem and at present we have only looked into the 1D case. In this section we will discuss the problems involved in finding relevant vacuum boundary conditions, and will give vacuum conditions for the 1D diffusion equation.

To impose vacuum conditions as given in (1.7), for the scalar flux we must integrate over Ω. However since the conditions are only specified for incoming angles, that integral is only defined over half its domain. In the 1D case this has been tackled in [13] (with the results more clearly given in [15] and [11]) by performing a boundary layer analysis in the neighbourhood of each end of the spatial domain. In each case a boundary layer expansion is matched to an interior expansion to obtain the condition. Though we do not fully understand this derivation yet, the resulting vacuum conditions are given in [15] as

$$\begin{aligned}\phi(a) - \Lambda\frac{\epsilon}{\hat{\sigma}_T}\frac{\partial}{\partial x}\phi(a) = 0,\\ \phi(b) + \Lambda\frac{\epsilon}{\hat{\sigma}_T}\frac{\partial}{\partial x}\phi(b) = 0,\end{aligned} \tag{3.24}$$

where

$$\Lambda \equiv \int_{[0,1]} \mu W(\mu)\,\mathrm{d}\mu \approx 0.710446, \tag{3.25}$$

and

$$W(\mu) \equiv \frac{\mu}{X(-\mu)}\left[\int_{[0,1]}\frac{\hat{\mu}}{X(-\hat{\mu})}\,\mathrm{d}\hat{\mu}\right]. \tag{3.26}$$

Values of $X(-\mu)$ are tabulated in [9], p.337. An alternative method for finding Λ for

the discrete case is given in [15], p.422, (and again in [11], p.1343).

3.3 Diffusion Synthetic Acceleration (DSA)

In this section, we will use the knowledge gained in Section 3.2 to show how the diffusion equation we derived can be used to choose the update required by Algorithm 2. In doing so we will form a method known as *diffusion synthetic acceleration*, or *DSA*, which we will then discuss. This method is discussed in [2], [3] and [23].

In Section 2.3 we noted that we want to choose the update, δ in Algorithm 2 such that

$$\delta^{(i+1/2)}(\mathbf{r}) \approx \phi(\mathbf{r}) - \phi^{(i+1/2)}(\mathbf{r}).$$

We also noted that an ideal method would be most accurate when σ_S is close to σ_T, since this is when source iteration has the potential for the slowest convergence. This is exactly the situation in which the diffusion equation, (3.20), should be the most accurate as an approximation to the transport equation. Therefore it seems a good idea to try to utilise this diffusion equation when finding the required update. With this in mind, we proceed.

First of all, let us denote by Σ the operation of multiplying by σ_S, so

$$\Sigma(\cdot) \equiv \left[\frac{\hat{\sigma}_T}{\epsilon} - \epsilon\hat{\sigma}_A\right](\cdot). \tag{3.27}$$

Using this, in Algorithm 2, step 2 solves

$$\mathcal{T}\psi^{(i+1/2)}(\mathbf{r},\Omega) = \Sigma\phi^{(i)}(\mathbf{r}) + Q(\mathbf{r}), \tag{3.28}$$

for $\psi^{i+1/2}(\mathbf{r},\Omega)$. Following the approach in the proof of Lemma 2.3, we subtract (3.28) from the transport equation (1.2) to obtain the error form

$$\mathcal{T}\left(\psi(\mathbf{r},\Omega) - \psi^{i+1/2}(\mathbf{r},\Omega)\right) = \Sigma\left(\phi(\mathbf{r}) - \phi^{i}(\mathbf{r})\right). \tag{3.29}$$

By adding and subtracting a scaling of the approximation $\phi^{i+1/2}(\mathbf{r},\Omega)$ from the right hand side, we can obtain

$$\mathcal{T}\left(\psi(\mathbf{r},\Omega) - \psi^{i+1/2}(\mathbf{r},\Omega)\right) = \Sigma\left(\phi(\mathbf{r}) - \phi^{i+1/2}(\mathbf{r})\right) + \Sigma\left(\phi^{i+1/2}(\mathbf{r}) - \phi^{i}(\mathbf{r})\right),$$

which, under our error definitions (2.11), can be written

$$\mathcal{T}e^{i+1/2}(\mathbf{r},\Omega) = \Sigma E^{i+1/2}(\mathbf{r}) + \Sigma\left(\phi^{i+1/2}(\mathbf{r}) - \phi^{i}(\mathbf{r})\right), \tag{3.30}$$

where $E^i(\mathbf{r}) \equiv \mathcal{P}e^i(\mathbf{r},\Omega)$ as in (2.11). Note here that an exact solution, $E^{i+1/2}(\mathbf{r})$, would make a perfect update for Algorithm 2. Also note that (3.30) can treated as a 3D transport equation where $e^{i+1/2}(\mathbf{r},\Omega)$ is the neutron flux, $E^{i+1/2}(\mathbf{r})$ is the scalar flux and $\Sigma\left(\phi^{i+1/2}(\mathbf{r}) - \phi^i(\mathbf{r})\right)$ is the source term. Consequently we can use the diffusion equation derived in Section 3.2 to approximate the error, $E^{i+1/2}(\mathbf{r})$, by solving

$$-\frac{1}{3\hat{\sigma}_T}\nabla\cdot\nabla E^{i+1/2}(\mathbf{r}) + \hat{\sigma}_A E^{i+1/2}(\mathbf{r}) = \frac{1}{\epsilon}\Sigma\left(\phi^{i+1/2}(\mathbf{r}) - \phi^i(\mathbf{r})\right), \tag{3.31}$$

where $E^{i+1/2}(\mathbf{r})$ satisfies the boundary conditions given in (3.24). We can then set $\delta^{i+1/2} = E^{i+1/2}$ in Algorithm 2, and the method is complete.

Using this particular method for obtaining the update causes Algorithm 2 to carry out the acceleration method known as *diffusion synthetic acceleration* that was mentioned in Section 1.3. For completeness we will include this algorithm in full here.

Algorithm 3: 3D Diffusion Synthetic Acceleration (DSA) [2]

1. Choose some initial $\phi^{(0)}(\mathbf{r})$,
2. solve
$$\mathcal{T}\psi^{(i+1/2)}(\mathbf{r},\Omega) = \Sigma\phi^{(i)}(\mathbf{r}) + Q(\mathbf{r}), \tag{3.32}$$
for $\psi^{(i+1/2)}(\mathbf{r},\Omega)$,
3. integrate to find $\phi^{(i+1/2)}(\mathbf{r}) = \mathcal{P}\psi^{(i+1/2)}(\mathbf{r},\Omega)$,
4. solve
$$-\frac{1}{3\hat{\sigma}_T}\nabla\cdot\nabla\delta^{i+1/2}(\mathbf{r}) + \hat{\sigma}_A\delta^{i+1/2}(\mathbf{r}) = \frac{1}{\epsilon}\Sigma\left(\phi^{i+1/2}(\mathbf{r}) - \phi^i(\mathbf{r})\right), \tag{3.33}$$
for $\delta^{i+1/2}(\mathbf{r})$,
5. update to find $\phi^{(i+1)}(\mathbf{r}) = \phi^{(i+1/2)}(\mathbf{r}) + \delta^{(i+1/2)}(\mathbf{r})$, and return to step 2.

In the coming chapters we will work primarily with the 1D transport equation and thus the appropriate algorithms and approximations. Consequently it is important to note that, as with the diffusion equation (3.20) itself, this algorithm can also be found for the one dimensional case. The derivation of the update follows exactly the procedure we used here.

3.4 Discussion

The diffusion equation derived in Section 3.2 is used in most reactor core simulations [23]. Before being applied however, the domain is frequently homogenised by averaging the cross sections spatially ([28] Chapter 3, p.47 and [23]). This is difficult to justify theoretically, however is necessary since the assumptions for a domain to be diffusive do not hold near material boundaries. The homogenisation process itself is not a unique process, and an open question remains about finding an optimal method. This is the source of one of the main limitations of the diffusion approximation, however accurate predictions can still be obtained by homogenising.

Unfortunately the assumptions for diffusivity are also violated close to the domain boundaries, and this cannot be resolved by working on a homogenised problem. It is for this reason that a boundary layer analysis is required to obtain relevant boundary conditions for the diffusion equation [13], [16]. However as an approximation to the scalar flux, the diffusion equation will be least accurate near the boundaries, and this can be observed numerically though we will not do so in the current report.

Chapter 4

Block Operator Form

4.1 Introduction

In this chapter, and for much of the remaining report, we will be working with the 1D transport equation, and with the appropriate associated equations and algorithms. Working in this setting has allowed us to develop the theory that will be presented, though it has made the work less physically relevant. In the future we aim to either extend our results back into a 3D space, or to understand why it is not possible to do so.

We have previously seen how the transport equation can be written in terms of operators, and that under certain conditions the scalar flux can be well approximated by a diffusion equation of the form (3.22). In Section 4.2 we will see how the transport equation can be written completely in a block operator format. Using this form we will demonstrate the link between the diffusion and transport equations.

4.2 Block Operator Transport Equation

In this section, we will show how the transport equation can be written in a block operator form.

Using (3.27) allows the transport equation to be written as

$$\mathcal{T}\psi(x,\mu) = \Sigma\phi(x) + \epsilon Q(x), \tag{4.1}$$

where

$$\phi(x) = \mathcal{P}\psi(x,\mu). \tag{4.2}$$

We can combine (4.1) and (4.2) into a block operator form as follows

$$\begin{pmatrix} \mathcal{T} & -\Sigma \\ -\mathcal{P} & \mathcal{I} \end{pmatrix} \begin{pmatrix} \psi \\ \phi \end{pmatrix} = \begin{pmatrix} \epsilon Q \\ 0 \end{pmatrix} \tag{4.3}$$

together with vacuum boundary conditions, (1.7), and where $\mathcal{I}$ is the identity operator ($\mathcal{I}(\cdot) \equiv (\cdot)$). From here we would like to see how the diffusion approximation, (3.22), is contained within this form. This will be our aim in Section 4.3.

4.3 Block Operator Diffusion Form

Having obtained the block operator form, (4.3), we would like to understand how the link seen in Section 3.2 between the transport and diffusion equations can be seen through this operator set up. To this end, we apply Gaussian elimination by premultiplying (4.3) as follows

$$\begin{aligned} &\begin{pmatrix} \mathcal{I} & 0 \\ \mathcal{P}\mathcal{T}^{-1} & \mathcal{I} \end{pmatrix} \begin{pmatrix} \mathcal{T} & -\Sigma \\ -\mathcal{P} & \mathcal{I} \end{pmatrix} \begin{pmatrix} \psi \\ \phi \end{pmatrix} = \begin{pmatrix} \mathcal{I} & 0 \\ \mathcal{P}\mathcal{T}^{-1} & \mathcal{I} \end{pmatrix} \begin{pmatrix} \epsilon Q \\ 0 \end{pmatrix} \\ \Rightarrow \quad &\begin{pmatrix} \mathcal{T} & -\Sigma \\ 0 & \mathcal{I} - \mathcal{P}\mathcal{T}^{-1}\Sigma \end{pmatrix} \begin{pmatrix} \psi \\ \phi \end{pmatrix} = \begin{pmatrix} \epsilon Q \\ \epsilon \mathcal{P}\mathcal{T}^{-1} Q \end{pmatrix}. \end{aligned}$$

Here we have obtained an equation purely in terms of the scalar flux, namely

$$(\mathcal{I} - \mathcal{P}\mathcal{T}^{-1}\Sigma)\phi = \epsilon \mathcal{P}\mathcal{T}^{-1} Q. \tag{4.4}$$

The operator, $\mathcal{I} - \mathcal{P}\mathcal{T}^{-1}\Sigma$, is a *Schur complement* form of the block operator matrix. Before proceeding with our analysis, we will prove symmetry of this operator on the Hilbert space $L^2(V)$.

Lemma 4.1:
The operator, $\mathcal{I} - \mathcal{P}\mathcal{T}^{-1}\Sigma$ mapping $L^2(V)$ to itself is a symmetric operator, i.e.

$$\left\langle (\mathcal{I} - \mathcal{P}\mathcal{T}^{-1}\Sigma) f, g \right\rangle_{L^2(V)} = \left\langle f, (\mathcal{I} - \mathcal{P}\mathcal{T}^{-1}\Sigma) g \right\rangle_{L^2(V)}, \tag{4.5}$$

for all $f, g \in L^2(V)$.

Proof.
In [27], Lemma 2.8, it is proved that $\mathcal{K}_{\sigma_T} (\equiv \mathcal{P}\mathcal{T}^{-1})$ is a symmetric operator on $L^2(V)$ in 1, 2 and 3D due to the symmetry of the kernal of $\mathcal{K}_{\sigma_T}$. We can use this to prove (4.5). Firstly since Σ is just scalar multiplication, we have

$$\begin{aligned} \left\langle (\mathcal{I} - \mathcal{P}\mathcal{T}^{-1}\Sigma) f, g \right\rangle_{L^2(V)} &= \langle \mathcal{I} f, g \rangle_{L^2(V)} - \left\langle \mathcal{P}\mathcal{T}^{-1}\Sigma f, g \right\rangle_{L^2(V)} \\ &= \langle \mathcal{I} f, g \rangle_{L^2(V)} - \Sigma \left\langle \mathcal{P}\mathcal{T}^{-1} f, g \right\rangle_{L^2(V)}. \end{aligned} \tag{4.6}$$

Now applying the result from [27] we can conclude

$$\begin{aligned}\left\langle (\mathcal{I}-\mathcal{P}\mathcal{T}^{-1}\Sigma)f, g\right\rangle_{L^2(V)} &= \langle \mathcal{I}f, g\rangle_{L^2(V)} - \Sigma\left\langle \mathcal{P}\mathcal{T}^{-1}f, g\right\rangle_{L^2(V)}. \\ &= \langle \mathcal{I}f, g\rangle_{L^2(V)} - \Sigma\left\langle f, \mathcal{P}\mathcal{T}^{-1}g\right\rangle_{L^2(V)}. \\ &= \left\langle f, (\mathcal{I}-\mathcal{P}\mathcal{T}^{-1}\Sigma)g\right\rangle_{L^2(V)}.\end{aligned} \tag{4.7}$$

□

If we could invert the Schur operator, $\mathcal{I}-\mathcal{P}\mathcal{T}^{-1}\Sigma$, then we could find the scalar flux exactly. However this is as difficult as solving the original transport equation. Instead, in the remainder of this section, we will build towards and prove two results which together show how (4.4) relates to the diffusion equation (3.22). First we will present two results that will be needed.

Lemma 4.2:

If

$$K(z) \equiv \frac{1}{2}\int_a^b \frac{1}{\mu}\exp\left(\frac{-|z|}{\mu}\right)\, d\mu \tag{4.8}$$

then

$$\int_{\mathbb{R}} K(z)\, dz = 1. \tag{4.9}$$

Proof.
The proof of this result is given in the Appendix, Section A.3. □

Lemma 4.3 (Fourier Integral Theorem)**:**
Let $f : \mathbb{R} \to \mathbb{R}$, and suppose that f is Lipschitz continuous and also globally bounded by some $\max_\xi |f(\xi)| \equiv C$. Suppose also we have some function $K : \mathbb{R} \to \mathbb{R}^+$ such that

$$\int_{\mathbb{R}} K(z)\, dz = \alpha,$$

where $\alpha \in \mathbb{R}$ is some constant. Then it holds that

$$\lim_{\delta\to 0}\frac{1}{\delta}\int_{\mathbb{R}} K\left(\delta^{-1}(x-y)\right) f(y)\, dy = f(x), \tag{4.10}$$

for all $x \in \mathbb{R}$.

Proof.
A proof of this result could not be found, and so we have presented one in the Appendix, Section A.3. □

Using Lemmas 4.2 and 4.3 we can now prove the following result.

Theorem 4.4:

Suppose you have a function $Q : [a, b] \to \mathbb{R}$ where $Q \in L^2([a, b])$, is Lipschitz continuous and has a global maximum. Suppose also that there is an extension $\tilde{Q} : \mathbb{R} \to \mathbb{R}$ of Q which maintains these properties over the whole real line, and is such that $\tilde{Q}\Big|_{[a,b]} \equiv Q$. Under the operator definitions (1.15) *it holds that*

$$\lim_{\epsilon \to 0} \frac{1}{\epsilon} \mathcal{P}\mathcal{T}^{-1} Q(x) = Q(x) \tag{4.11}$$

pointwise, for all $x \in (a, b)$.

Proof.
Under the definitions given in F. Scheben [27], Lemma 2.3 in a 1D setting, we are interested in the behaviour of $\epsilon^{-1}\mathcal{K}_{\epsilon^{-1}} Q(x)$ as $\epsilon \to 0$. Using [27], (2.16), we know

$$\epsilon^{-1}\mathcal{K}_{\delta^{-1}} Q(x) = \frac{1}{\epsilon} \int_{[a,b]} K\left(\epsilon^{-1}(x - y)\right) Q(y) \, \mathrm{d}y \tag{4.12}$$

where

$$K(z) = \frac{1}{2} \int_{[a,b]} \frac{1}{\mu} \exp\left(\frac{-|z|}{\mu}\right) \mathrm{d}\mu.$$

Let us begin by splitting the integral in (4.12) into two domains

$$\begin{aligned} \frac{1}{\epsilon} \int_{[a,b]} K\left(\epsilon^{-1}(x - y)\right) Q(y) \, \mathrm{d}y = \frac{1}{\epsilon} \int_{\mathbb{R}} K\left(\epsilon^{-1}(x - y)\right) \tilde{Q}(y) \, \mathrm{d}y - \\ \underbrace{\frac{1}{\epsilon} \int_{\mathbb{R} \setminus [a,b]} K\left(\epsilon^{-1}(x - y)\right) \tilde{Q}(y) \, \mathrm{d}y}_{\equiv I}. \end{aligned} \tag{4.13}$$

By Lemma 4.3 we have that

$$\frac{1}{\epsilon} \int_{\mathbb{R}} K\left(\epsilon^{-1}(x - y)\right) \tilde{Q}(y) \, \mathrm{d}y \to \tilde{Q}(x) = Q(x), \quad \forall x \in (a, b) \text{ as } \epsilon \to 0. \tag{4.14}$$

It remains to show that $I \to 0$ with ϵ. To do this we look at the two halves of the domain of integration of I in turn

$$I = \underbrace{\frac{1}{\epsilon} \int_{(b,\infty)} K\left(\epsilon^{-1}(x - y)\right) \tilde{Q}(y) \, \mathrm{d}y}_{\equiv I^+} + \underbrace{\frac{1}{\epsilon} \int_{(-\infty,a)} K\left(\epsilon^{-1}(x - y)\right) \tilde{Q}(y) \, \mathrm{d}y}_{\equiv I^-}. \tag{4.15}$$

First of all, applying the change of variables $z = \epsilon^{-1}(x-y)$, we get

$$\begin{aligned} |I^+| &= \left| \frac{1}{\epsilon}(-\epsilon) \int_{(\epsilon^{-1}(x-b),-\infty)} K(z)\tilde{Q}(x-\epsilon z)\, \mathrm{d}z \right| \\ &= \left| \int_{(-\infty,\epsilon^{-1}(x-b))} K(z)\tilde{Q}(x-\epsilon z)\, \mathrm{d}z \right|. \end{aligned} \tag{4.16}$$

We can now use the fact that $\tilde{Q}$ has a global bound to get

$$|I^+| \leq \left\| \tilde{Q} \right\|_{\infty,[a,b]} \int_{(-\infty,\epsilon^{-1}(x-b))} K(z)\, \mathrm{d}z. \tag{4.17}$$

This tends to zero with ϵ provided that $x \in [a,b)$. Using an equivalent argument we can also find that $|I^-| \to 0$ as $\epsilon \to 0$ provided that $x \in (a,b]$. Thus taking $x \in (a,b)$ satisfies both conditions and the proof is complete. □

We now prove a result relating to the inverse operator, $\mathcal{T}^{-1} : L^2([a,b], L^1[-1,1]) \to L^2([a,b], L^1[-1,1])$, as the inverse of $\mathcal{T} : L^2([a,b], L^1[-1,1]) \to L^2([a,b], L^1[-1,1])$ with vacuum boundary conditions. I.e. $w(x,\mu) \equiv \mathcal{T}^{-1}g(x,\mu)$ solves

$$\mathcal{T}w(x,\mu) = g(x,\mu),$$

and also satisfies vacuum boundary conditions, as given by (1.13), for all $w, g \in L^2([a,b], L^1[-1,1])$. This result will be useful later.

Lemma 4.5:
Under the definition of $\mathcal{T}^{-1} : L^2([a,b], L^1[-1,1]) \to L^2([a,b], L^1[-1,1])$ given in [27], (2.14), it holds that

$$\mathcal{T}^{-1}(f(\mu)h(x)) = f(\mu)\mathcal{T}^{-1}h(x). \tag{4.18}$$

where $f \in L^1[-1,1]$ and $h \in L^2[a,b]$.

Proof.
In [27], (2.14), the inverse operator $\mathcal{T}^{-1}$ is defined as

$$\left(\mathcal{T}^{-1}g\right)(x,\mu) = \begin{cases} \frac{1}{\mu}\int_a^x \exp\left(\frac{\hat{\sigma}_T}{\epsilon\mu}(t-x)\right) g(t,\mu)\, \mathrm{d}t\,, & \text{if } \mu > 0 \\ -\frac{1}{\mu}\int_x^b \exp\left(\frac{\hat{\sigma}_T}{\epsilon\mu}(t-x)\right) g(t,\mu)\, \mathrm{d}t\,, & \text{if } \mu < 0. \end{cases} \tag{4.19}$$

where $g \in L^2([a,b], L^1[-1,1])$. If we can separate $g(x,\mu) \equiv f(\mu)h(x)$ then

$$\mathcal{T}^{-1}f(\mu)h(x) = \begin{cases} \frac{1}{\mu}\int_a^x \exp\left(\frac{\hat{\sigma}_T}{\epsilon\mu}(t-x)\right) f(\mu)h(t)\ \mathrm{d}t\ , & \text{if } \mu > 0 \\ -\frac{1}{\mu}\int_x^b \exp\left(\frac{\hat{\sigma}_T}{\epsilon\mu}(t-x)\right) f(\mu)h(t)\ \mathrm{d}t\ , & \text{if } \mu < 0. \end{cases}$$

Taking $f(\mu)$ outside leaves

$$\mathcal{T}^{-1}(f(\mu)h(x)) = f(\mu)\mathcal{T}^{-1}h(x). \tag{4.20}$$

□

Using this we will prove a result concerning the convergence of the Schur operator on the left side of (4.4). The proof of this result is not yet complete, and we have included the area of weakness as an assumption so that the result we state here is still valid.

Theorem 4.6 (Diffusion Approximation Theorem)**:**
If we know that at worst

$$\mathcal{P}\mu^{k+1}\mathcal{T}^{-1}\frac{d^{k+1}}{dx^{k+1}}\phi(x) \sim O(\epsilon^{-(k-3)}) \tag{4.21}$$

then it holds that

$$\frac{\hat{\sigma}_T}{\epsilon^2}(\mathcal{I} - \mathcal{P}\mathcal{T}^{-1}\Sigma)\phi(x) = \frac{-1}{3\hat{\sigma}_T}\frac{d^2}{dx^2}\phi(x) + \hat{\sigma}_A\phi(x) + O(\epsilon). \tag{4.22}$$

Proof.
We know

$$\begin{aligned} \mathcal{T} &= \mu\frac{\partial}{\partial x} + \frac{\hat{\sigma}_T}{\epsilon}I \\ &= \frac{\hat{\sigma}_T}{\epsilon}\left(\mathcal{I} + \frac{\epsilon\mu}{\hat{\sigma}_T}\frac{\partial}{\partial x}\right) \end{aligned} \tag{4.23a}$$

$$\Sigma = \left[\frac{\hat{\sigma}_T}{\epsilon} - \hat{\sigma}_A\epsilon\right] I. \tag{4.23b}$$

Now note that, for any arbitrary operator $\mathcal{A}$, it holds that

$$(\mathcal{I} + \mathcal{A})^{-1} = \mathcal{I} - \mathcal{A} + \mathcal{A}^2 - \cdots - \mathcal{A}^k - (\mathcal{I} + \mathcal{A})^{-1}\mathcal{A}^{k+1}. \tag{4.24}$$

Applying this to (4.23a) we get

$$\begin{aligned}\mathcal{T}^{-1} &= \frac{\epsilon}{\hat{\sigma}_T}\left(I + \frac{\epsilon\mu}{\hat{\sigma}_T}\frac{\partial}{\partial x}\right)^{-1}, \\ &= \underbrace{\frac{\epsilon}{\hat{\sigma}_T}\left(I - \frac{\epsilon\mu}{\hat{\sigma}_T}\frac{\partial}{\partial x} + \frac{\epsilon^2\mu^2}{\hat{\sigma}_T^2}\frac{\partial^2}{\partial x^2} - \cdots - \frac{\epsilon^k\mu^k}{\hat{\sigma}_T^k}\frac{\partial^k}{\partial x^k}\right)}_{\equiv(*)} - \underbrace{\mathcal{T}^{-1}\frac{\epsilon^{k+1}\mu^{k+1}}{\hat{\sigma}_T^{k+1}}\frac{\partial^{k+1}}{\partial x^{k+1}}}_{\equiv\mathcal{E}}\end{aligned}$$

Now considering just $(*)$ with (4.23b) we find

$$\begin{aligned}\mathcal{P}(*)\Sigma &= \frac{\epsilon}{\hat{\sigma}_T}\mathcal{P}\left(I - \frac{\epsilon\mu}{\hat{\sigma}_T}\frac{\partial}{\partial x} + \frac{\epsilon^2\mu^2}{\hat{\sigma}_T^2}\frac{\partial^2}{\partial x^2} - \cdots - \frac{\epsilon^k\mu^k}{\hat{\sigma}_T^k}\frac{\partial^k}{\partial x^k}\right)\Sigma, \\ &= \left[\mathcal{I} - \frac{\epsilon^2\hat{\sigma}_A}{\hat{\sigma}_T}\right]\left(\mathcal{P} - \frac{\epsilon}{\hat{\sigma}_T}\frac{\mathrm{d}}{\mathrm{d}x}\mathcal{P}\mu + \frac{\epsilon^2}{\hat{\sigma}_T^2}\frac{\mathrm{d}^2}{\mathrm{d}x^2}\mathcal{P}\mu^2 - \cdots - \frac{\epsilon^k}{\hat{\sigma}_T^k}\frac{\partial^k}{\partial x^k}\mathcal{P}\mu^k\right).\end{aligned}$$

If we note that $\mathcal{P}\phi = \phi$, and that

$$\mathcal{P}\mu^i = \begin{cases} 0\ , & \text{for } i \text{ odd} \\ \frac{1}{i+1}, & \text{for } i \text{ even} \end{cases},$$

then we find

$$(\mathcal{P}(*)\Sigma)\phi = \phi + \frac{\epsilon^2}{3\hat{\sigma}_T^2}\frac{\mathrm{d}^2}{\mathrm{d}x^2}\phi - \frac{\epsilon^2\hat{\sigma}_A}{\hat{\sigma}_T}\phi + O(\epsilon^4). \tag{4.25}$$

Including $\mathcal{E}$ once more we find

$$(\mathcal{I} - \mathcal{P}\mathcal{T}^{-1}\Sigma)\phi = -\frac{\epsilon^2}{3\hat{\sigma}_T^2}\frac{\mathrm{d}^2}{\mathrm{d}x^2}\phi + \frac{\epsilon^2\hat{\sigma}_A}{\hat{\sigma}_T}\phi - O(\epsilon^4) + \mathcal{P}\mathcal{E}\Sigma\phi. \tag{4.26}$$

Scaling by $\hat{\sigma}_T/\epsilon^2$ (as in (4.22)) leaves

$$\frac{\hat{\sigma}_T}{\epsilon^2}(\mathcal{I} - \mathcal{P}\mathcal{T}^{-1}\Sigma)\phi = -\frac{1}{3\hat{\sigma}_T}\frac{\mathrm{d}^2}{\mathrm{d}x^2}\phi + \hat{\sigma}_A\phi - O(\epsilon^2) + \frac{\hat{\sigma}_T}{\epsilon^2}\mathcal{P}\mathcal{E}\Sigma\phi. \tag{4.27}$$

To establish the desired result it remains to verify that at least $\frac{\hat{\sigma}_T}{\epsilon^2}\mathcal{P}\mathcal{E}\Sigma\phi \sim O(\epsilon)$. Just from definitions we have

$$\begin{aligned}\mathcal{P}\mathcal{E}\Sigma\phi(x) &= \mathcal{P}\mathcal{T}^{-1}\frac{\epsilon^{k+1}\mu^{k+1}}{\hat{\sigma}_T^{k+1}}\frac{\mathrm{d}^{k+1}}{\mathrm{d}x^{k+1}}\left[\frac{\hat{\sigma}_T}{\epsilon} - \epsilon\hat{\sigma}_A\right]\phi(x) \\ &= \mathcal{P}\left(\mathcal{T}^{-1}\frac{\epsilon^k\mu^{k+1}}{\hat{\sigma}_T^k}\frac{\mathrm{d}^{k+1}}{\mathrm{d}x^{k+1}}\phi(x) - \mathcal{T}^{-1}\frac{\epsilon^{k+2}\mu^{k+1}}{\hat{\sigma}_T^{k+2}}\frac{\mathrm{d}^{k+1}}{\mathrm{d}x^{k+1}}\phi(x)\right).\end{aligned} \tag{4.28}$$

Applying Lemma 4.5 twice leaves

$$\mathcal{P}\mathcal{E}\Sigma\phi(x) = \left[\frac{\epsilon^k}{\hat{\sigma}_T^k} - \frac{\epsilon^{k+2}}{\hat{\sigma}_T^{k+2}}\right]\mathcal{P}\mu^{k+1}\mathcal{T}^{-1}\frac{\mathrm{d}^{k+1}}{\mathrm{d}x^{k+1}}\phi(x). \tag{4.29}$$

The order of $\frac{\hat{\sigma}_T}{\epsilon^2}\mathcal{P}\mathcal{E}\Sigma\phi$ is therefore governed by the order of

$$\frac{\epsilon^{k-2}}{\hat{\sigma}_T^{k-1}}\mathcal{P}\mu^{k+1}\mathcal{T}^{-1}\frac{\mathrm{d}^{k+1}}{\mathrm{d}x^{k+1}}\phi(x). \tag{4.30}$$

From our assumption, (4.21), we know that this is at least $O(\epsilon)$, and so our proof is complete. □

So in summary: we have proved two results in Theorems 4.4 and 4.6 which together show that, under certain assumptions, the limit as $\epsilon \to 0$ of a suitable scaling of the operator equation (4.4) is the diffusion equation (3.22) defined on the interior of the spatial domain, i.e. $x \in (a, b)$. In Chapter 5 we will look at a discretised block-matrix form of the transport equation, and consider how these results influence the method of diffusion synthetic acceleration, introduced in Chapter 3.

Chapter 5

Block Matrix Form

5.1 Introduction

In Chapter 4 we saw how the operator transport equation (1.16) can be written in a block operator format as (4.3). We went on to prove results that linked an easily obtainable operator equation, (4.4), with the diffusion approximation (3.22) in the limit as $\epsilon \to 0$.

In this chapter we will explore what the theory from Chapter 4 implies for a discretised version of the transport equation. To do this, we will also look at how Algorithm 2, and the update established in Section 3.3, can be understood from this point of view.

We start by exploring one possible discretisation of the one dimensional transport equation, (1.12).

5.2 Discretising the 1D Transport Equation

In this section we look at how the 1D transport equation, (1.12), can be discretised in space and angle, allowing for approximate discrete solutions to be found. The method we will focus on was mentioned briefly in Section 1.3 (where relevant literature was mentioned), and is called the method of *discrete ordinates*. The fundamental idea of the method is to sample the angular variable, μ, at a number discrete points and to then replace integrals over angle by weighted quadrature sums. Here we will choose the angles to be Gauss-Jacobi quadrature points on $[-1, 1]$ (see [1], Section 25.4.33, and [24] for Gauss-Jacobi quadrature). Specifically we will choose

$$\mu_k \in [-1, 1], |k| = 1, \ldots, N, \text{ such that } \mu_k = -\mu_{-k},$$

with associated weights

$$\omega_k \in \mathbb{R}, |k| = 1, \ldots, N, \text{ such that } \omega_k = \omega_{-k}.$$

Note that we have taken an even number of quadrature points, meaning all the points μ_k are non-zero. Using this discretisation, we can write the definition of the scalar flux, (4.2), as a quadrature summation

$$\phi(x) = \mathcal{P}\psi(x,\mu) \approx \frac{1}{2}\sum_{|k|=1,\ldots,N} \omega_k \psi(x,\mu_k). \tag{5.1}$$

To discretise in space one simple method is that of *diamond differencing* in which derivatives are replaced by difference equations, and function values at each node are set to equal the average of their values at the surrounding nodes. We discretise the spatial domain as follows

$$a \equiv x_0 < x_1 < \cdots < x_M \equiv b, \text{ with } |x_k - x_{k-1}| = h. \tag{5.2}$$

We will use the notation

$$\begin{aligned} \psi(x_j,\mu_k) &\equiv \psi_{j,k} \\ \phi(x_j) &\equiv \phi_j \end{aligned} \tag{5.3}$$

to simplify the exposition that is to come. With this spatial discretisation, we will replace derivatives in x by

$$\frac{\partial}{\partial x}\psi_{j+1/2,k} \approx \frac{\psi_{j+1,k} - \psi_{j,k}}{h} \tag{5.4}$$

Under these discretisations and using this notation, we can write the one dimensional transport equation, (3.23), as

$$\mu_k \frac{\psi_{j+1,k} - \psi_{j,k}}{h} + \frac{\hat{\sigma}_T}{\epsilon}\frac{\psi_{j+1,k} + \psi_{j,k}}{2} = \left[\frac{\hat{\sigma}_T}{\epsilon} - \epsilon\hat{\sigma}_A\right]\phi_{j+1/2} + q_{j+1/2}, \tag{5.5}$$

for $j = 0,\ldots,M-1$ and $|k| = 1,\ldots,N$, where

$$\phi_{j+1/2} \equiv \frac{1}{2}\sum_{|k|=1,\ldots,N} \omega_k \frac{\psi_{j+1,k} + \psi_{j,k}}{2}, \tag{5.6}$$

In (5.5) there are $2NM$ equations and $2N(M+1)$ unknowns, thus we require boundary conditions to find a unique solution. We can easily discretise the boundary conditions given in Section 1.2 and say that under vacuum boundary conditions we include the equations

$$\begin{aligned} \psi_{M,k} &= 0, \; -N \le k < 0, \\ \psi_{0,k} &= 0, \quad 0 < k \le N. \end{aligned} \tag{5.7}$$

Alternatively, under reflecting boundary conditions we would include

$$\left.\begin{aligned}\psi_{M,k} &= \psi_{M,-k} \\ \psi_{0,k} &= \psi_{0,-k}\end{aligned}\right\} 0 < k \leq N. \tag{5.8}$$

Combining either set of boundary conditions with (5.5) leads to a consistent and uniquely solvable system of equations.

5.3 1D Matrix Transport Equation

In this section we will show how the discrete system found in Section 5.2 can be written in a matrix format. Following the matrix formulation presented in [7] and [12] leaves us with the matrices

- $T \in \mathbb{R}^{2N(M+1)\times 2N(M+1)}$ representing the transport operator, $\mathcal{T}$. Specifies vacuum boundary conditions together with Q.
- $\Sigma \in \mathbb{R}^{2N(M+1)\times M}$ representing the operator Σ,
- $P \in \mathbb{R}^{M\times 2N(M+1)}$ representing the operator $\mathcal{P}$,
- $Q \in \mathbb{R}^{2N(M+1)\times 1}$ representing the non-fission source, $Q(x)$. Specifies vacuum boundary conditions together with T.

Despite some crossover of notation between some matrices and their corresponding operators, it should be clear from context which of the two is meant. We also have the unknown vectors

- $\Psi \in \mathbb{R}^{2N(M+1)}$ representing the neutron flux, $\psi(x,\mu)$,
- $\Phi \in \mathbb{R}^{M}$ representing the scalar flux, $\phi(x)$.

This set-up allows for the discrete transport equation to be written as

$$T\Psi = \Sigma\Phi + \epsilon Q, \tag{5.9}$$

where

$$\Phi = P\Psi.$$

To solve this, we could employ the following discrete matrix version of source iteration

Algorithm 4: Matrix Source Iteration

- Choose Φ^0,
- Solve
$$T\Psi^{i+1} = \Sigma\Phi^i + \epsilon Q, \tag{5.10}$$
- Find $\Phi^{i+1} = P\Psi^{i+1}$, and repeat.

We can prove convergence of source iteration in matrix form, however we must make a couple of assumptions which will discuss afterwards.

Lemma 5.1:
If the matrix $PT^{-1}\Sigma$ is a real symmetric matrix, and has maximum eigenvalue that satisfies $\lambda_{max}(PT^{-1}\Sigma) \sim 1 - O(\epsilon^2)$, then Algorithm 4 converges.

Proof.
If we define two matrix errors as

$$\mathbf{e}^i \equiv \Psi - \Psi^i,$$
$$\mathbf{E}^i \equiv \Phi - \Phi^i,$$

then subtracting (5.10) from (5.9) leaves

$$T\mathbf{e}^{i+1} = \Sigma\mathbf{E}^i. \tag{5.11}$$

Premultiplying by PT^{-1} give us

$$\mathbf{E}^{i+1} = PT^{-1}\Sigma\mathbf{E}^i, \tag{5.12}$$

and so

$$\begin{aligned} \left\|\mathbf{E}^{i+1}\right\|_2 &= \left\|PT^{-1}\Sigma\mathbf{E}^i\right\|_2 \\ &\leq \left\|PT^{-1}\Sigma\right\|_2 \left\|\mathbf{E}^i\right\|_2, \end{aligned} \tag{5.13}$$

where

$$\|A\|_2 \equiv \sqrt{\lambda_{max}(A^*A)} \tag{5.14}$$

and A^* denotes the conjugate transpose of A. If A is a real symmetric matrix, i.e. $A^* = A$, then $A^*A = A^2$ and so

$$\begin{aligned} \lambda_{max}\left(A^*A\right) &= \lambda_{max}\left(A^2\right) \\ &= \lambda_{max}\left(A\right)^2. \end{aligned}$$

Therefore for real symmetric matrices, A, (5.14) becomes

$$\|A\|_2 \equiv \lambda_{max}(A). \tag{5.15}$$

Since $(PT^{-1}\Sigma)$ is real and symmetric, we have that

$$\left\|(PT^{-1}\Sigma)\right\|_2 = \lambda_{max}(PT^{-1}\Sigma) \sim 1 - O(\epsilon^2). \tag{5.16}$$

Combining this with (5.13) yields the result. □

The two assumptions made in this proof are supported by numerical experiment. However at this point proofs have not been found for the discrete case. In fact, the behaviour that can be observed numerically appears to show

$$\begin{aligned} \lambda_{max}(PT^{-1}\Sigma) &\sim 1 - O(\epsilon^2) \\ \lambda_{min}(PT^{-1}\Sigma) &\sim 1 - O(\epsilon). \end{aligned} \tag{5.17}$$

In the next section we will go further with the idea of a matrix transport equation, and form a discrete equivalent to (4.3).

5.4 1D Block Matrix Transport Equation

In Section 4.2 a block operator version of the transport equation, (4.3), was given. In this section we will give the discrete equivalent to that equation, and consider what the analysis from Section 4.3 can tell us about the discrete case.

So firstly, a discretised block matrix version of the 1D transport equation is given by

$$\begin{pmatrix} T & -\Sigma \\ -P & I \end{pmatrix} \begin{pmatrix} \Psi \\ \Phi \end{pmatrix} = \begin{pmatrix} \epsilon Q \\ 0 \end{pmatrix}. \tag{5.18}$$

Applying Gaussian elimination to mimic what was done in Section 4.3 we proceed

$$\begin{aligned} & \begin{pmatrix} I & 0 \\ PT^{-1} & I \end{pmatrix} \begin{pmatrix} T & -\Sigma \\ -P & I \end{pmatrix} \begin{pmatrix} \Psi \\ \Phi \end{pmatrix} = \begin{pmatrix} I & 0 \\ PT^{-1} & I \end{pmatrix} \begin{pmatrix} \epsilon Q \\ 0 \end{pmatrix}. \\ \Rightarrow \quad & \begin{pmatrix} \mathcal{T} & -\Sigma \\ 0 & \mathcal{I} - \mathcal{P}\mathcal{T}^{-1}\Sigma \end{pmatrix} \begin{pmatrix} \Psi \\ \Phi \end{pmatrix} = \begin{pmatrix} \epsilon Q \\ \epsilon PT^{-1}Q \end{pmatrix}. \end{aligned} \tag{5.19}$$

Once again, this gives us an equation for the scalar flux, as

$$(I - PT^{-1}\Sigma)\Phi = \epsilon PT^{-1}Q. \tag{5.20}$$

where the Schur complement $(I - PT^{-1}\Sigma)$ is a dense $M \times M$ real matrix. Inverting it

would solve for Φ, however it would also take $O(M^3)$ operations, and so be prohibitively expensive for finer discretisations. Instead we would like to approximate (5.20) with something more easily solvable.

For this we turn to the theory developed in Section 4.3, specifically Theorems 4.4 and 4.6. These tell us that it is possible to approximate a $\hat{\sigma}_T/\epsilon^2$ scaling of (5.20) using the diffusion equation (3.22). Once discretised, the diffusion equation can be written as a tridiagonal matrix-vector equation. Consequently it can then be solved using Gaussian elimination (specifically the Thomas algorithm) in only $O(M)$ operations.

In Chapter 6 we will present some numerical results. To obtain these we wrote programs that use the discretisation given in Section 5.2 to form the matrices used in Section 5.3.

Chapter 6

Numerical Tests

6.1 Introduction

In this chapter we will have a look at the results of some numerical tests based around results and ideas presented in this report. We will work solely in 1D.

Firstly, Section 6.2 will look at the convergence of source iteration (Algorithm 1 in 1D) without an update. Next Section 6.3 will look at how well the diffusion equation performs on its own as an approximation to the transport equation. Lastly, Section 6.4 will look at the convergence of DSA (Algorithm 3 in 1D).

6.2 1D Source Iteration

In this section we will solve the transport equation using source iteration for various values of ϵ. We will see that as ϵ decreases, source iteration takes a greater number of iterations to converge. This is the behaviour predicted by Lemma 2.4 (in 1D Lemma A.4) and we will go on to compare more precisely how the observed behaviour reflects what was predicted.

For this experiment, we wrote a 1D code using the discretisation and matrix set-up described in Section 5.2. We will use $x \in [0, 1]$, with $\hat{\sigma}_T = \hat{\sigma}_A = 1$, and also $q(x) = 1, \forall x \in [0, 1]$. Using the notation from Section 5.2, we will chose $M = N = 256$. This means that if we formed the block matrix system, (5.18), it would be a 131840×131840 square matrix. We will vary ϵ in steps of 0.2 from 1 down to 0.2, and use an initial guess of the zero vector for ϕ^0 each time. To measure convergence, we will use the 2-norm of the difference between a benchmark solution and our current approximation. This benchmark solution will be found by directly solving the full linear system of equations, (i.e. (5.18)).

Following these guides, we obtain the following table of errors.

Iteration	ϵ				
	1.0	0.8	0.6	0.4	0.2
1	1.4e-014	2.2e+000	3.8e+000	4.7e+000	4.7e+000
2		5.3e-001	1.8e+000	3.3e+000	4.2e+000
3		1.3e-001	8.6e-001	2.3e+000	3.7e+000
⋮		⋮	⋮	⋮	⋮
17		3.2e-010	2.6e-005	1.4e-002	7.3e-001
18		7.8e-011	1.2e-005	9.8e-003	6.5e-001
19			5.9e-006	6.8e-003	5.8e-001
20			2.8e-006	4.7e-003	5.2e-001
⋮			⋮	⋮	⋮
33			1.8e-010	4.2e-005	1.2e-001
34			8.5e-011	2.9e-005	1.0e-001
35				2.0e-005	9.2e-002
36				1.4e-005	8.2e-002
⋮				⋮	⋮
68				1.2e-010	2.0e-003
69				8.6e-011	1.8e-003
70					1.6e-003
71					1.4e-003
⋮					⋮
213					1.1e-010
214					9.6e-011

Table 6.1: *Error in source iteration obeserved at each iteration for varying ϵ.*

Clearly as ϵ decreases source iteration is requiring more iterations to converge. Lemma 2.4 bounds the ratio between successive errors to be no more that σ_S/σ_T. This doesn't prevent source iteration from converging rapidly in any situation, however it says there is the potential for slow convergence in some cases. To see how close this ratio is to the observed ratio, we give the following table.

	ϵ				
	1.0	0.8	0.6	0.4	0.2
Predicted ratio, $\left(\frac{\sigma_S}{\sigma_T}\right)$	0	0.36	0.64	0.84	0.96
Observed ratio	—	0.2427	0.4756	0.6950	0.8909

Table 6.2: *Observed ratios versus predicted ratios in successive errors in source iteration, for varying values of ϵ.*

Thus, while source iteration is outperforming the predicted 'worst case', it is still showing reduced performance for smaller ϵ.

For even smaller values of ϵ, source iteration quickly becomes unfeasible. Solving with a much coarser discretisation of $M = N = 16$, and taking $\epsilon = 10^{-3}$ takes 4241608 iterations to converge to an error of 10^{-8}.

While this method is very basic it is nonetheless interesting to analyse and is still very relevant as it is used in industry-standard neutron transport codes.

6.3 1D Diffusion Equation

In this section we will will look at how well the diffusion equation, (3.22), can approximate the true scalar flux for varying values of ϵ. We will do this by directly solving both the discrete diffusion equation in matrix form (via the Thomas algorithm) and the full linear system of equations, (5.18), and then looking at the 2-norm of the difference of the two solutions. We will see that as ϵ decreases the norm of the difference decreases, as predicted by the theory in Chapter 3 and by Theorem 4.6. However for very small values of ϵ (beyond $\epsilon = 10^{-5}$) the norm of the difference increases. We will discuss why this might happen.

For this experiment, we wrote a 1D diffusion solver using the same spatial discretisation as presented in Section 5.2. We will use the same set-up as in Section 6.2, but we will vary ϵ in powers of 10 from $\epsilon = 10^{-1}$ down to $\epsilon = 10^{-8}$.

Doing this we obtain the following table of errors.

	ϵ							
	10^{-1}	10^{-2}	10^{-3}	10^{-4}	10^{-5}	10^{-6}	10^{-7}	10^{-8}
$\|\phi_{\text{diff}} - \phi_{\text{tran}}\|_2$	5e-02	2e-03	1e-04	3e-05	9e-06	4e-03	4e-01	3e+00

Table 6.3: *Norm of the difference between scalar flux solutions found using the transport and diffusion methods for varying values of ϵ.*

Here we have used ϕ_{diff} and ϕ_{tran} to denote the diffusion and transport solutions respectively. For ϵ greater than 10^{-5} the error seems to decrease with $O(\epsilon)$, as could

be expected from Theorem 4.6. However for $\epsilon = 10^{-6}$ and smaller, the error increases once more. This behaviour will also be apparent in the results in Section 6.4, and we will now examine it further.

We will first look at the convergence of the scalar flux solution found as ϵ decreases, for each solution method. If we denote by $\phi^{[k]}$ the solution for $\epsilon = 10^{-k}$, then we shall consider

$$\left\| \phi^{[k]} - \phi^{[k+1]} \right\|_2,$$

for $k = 1, \ldots, 8$. These values are given in the following table.

k	$\left\| \phi^{[k]}_{\text{diff}} - \phi^{[k+1]}_{\text{diff}} \right\|_2$	$\left\| \phi^{[k]}_{\text{tran}} - \phi^{[k+1]}_{\text{tran}} \right\|_2$
1	9e-001	1e+000
2	1e-001	1e-001
3	1e-002	1e-002
4	1e-003	1e-003
5	1e-004	4e-003
6	1e-005	4e-001
7	1e-006	3e+000

Table 6.4: *Norm of the difference between solutions, ϕ, found for successive powers of ϵ. Contains data for transport and diffusion solves.*

These show that to begin with, the solutions found by both the diffusion and transport methods are converging as $\epsilon \to 0$ (though not necessarily to each other). However while ϕ_{diff} maintains this behaviour for all ϵ we tested, ϕ_{tran} does not. In fact, it is for $k = 6$ that the convergence starts to break, which is when the transport solution found for $\epsilon = 10^{-6}$ is first considered. This fits the behaviour shown in Table 6.3 and though it doesn't explain it, it suggests that the error may be caused by the transport and not the diffusion solve.

Next we look at the exact 1D transport equation being solved, which we restate here, and we will present an heuristic argument to explain the behaviour.

$$\mu \frac{\partial}{\partial x}\psi(x,\mu) + \frac{\hat{\sigma}_T}{\epsilon}\psi(x,\mu) = \left[\frac{\hat{\sigma}_T}{\epsilon} - \epsilon\hat{\sigma}_A\right]\phi(x) + \epsilon Q(x). \tag{6.1}$$

In this equation there are $O(\epsilon^{-1})$, $O(\epsilon^0)$ and $O(\epsilon^1)$ terms. Consequently some terms differ by two orders of magnitude in ϵ. As $\epsilon \to 0$, the $O(\epsilon^{-1})$ terms will dominate, and in the limit the equation will simply be saying that $\psi(x,\mu) = \phi(x)$ (as mentioned in Chapter 3). But we are not working in the limit, and the influence of the higher-order terms is important in capturing the transport behaviour that we want to model.

Unfortunately we are working in double-precision arithmetic, so differences greater than $O(10^{16})$ will be lost, and differences of order close to $O(10^{16})$ will become inaccurate particularly over the course of an iterative method. In the case of the transport equation for a value of $\epsilon = 10^{-k}$, some terms differ by an order of $O(10^{2k})$, and so you could not expect to improve the accuracy of the solution beyond an error of about $10^{-(16-2k)}$. (This lower bound on the error will be seen almost exactly in the case of DSA in Section 6.4.)

If this is the case, we expect that for values of $\epsilon < 10^{-8}$, our transport code would begin to solve the limiting equation, $\psi(x, \mu) = \phi(x)$. The trivial solution to this is zero, so we might expect to see the solution converge to zero with ϵ. This is indeed what is seen, and the following table contains the norm of the solution ϕ_{tran} obtained for several values of ϵ.

	ϵ						
	10^{-5}	10^{-6}	10^{-7}	10^{-8}	10^{-9}	10^{-10}	10^{-11}
$\|\phi_{\text{tran}}\|_2$	3.36	3.36	3.00	2.58e-01	3.11e-03	3.10e-05	3.15e-07

Table 6.5: *Norm of the scalar flux solution found using a transport solve for varying values of ϵ.*

In conclusion, the above heuristic argument implies that the accuracy of the solution to the non-dimensional 1D transport equation, (3.23), is being limited by the machine precision. To verify that this is the case we could try working in single precision instead, to see if an equivalent (albeit worse) accuracy bound is seen. If it is, then it would be sensible to move away from MATLAB and instead use a programming language which allows arbitrary precision, such as fortran or maple.

6.4 1D Diffusion Synthetic Acceleration

In this section we explore how much the acceleration method DSA speeds up the convergence of source iteration (the convergence of which was seen in Section 6.2) for various values of ϵ. We will also look at the convergence behaviour it does display in ϵ, and ask whether this agrees with the knowledge we have gained so far.

For this experiment, we wrote a 1D version of Algorithm 3 using the discretisation described in Section 5.2 for the transport equation, and we used an equivalent spatial discretisation for the diffusion equation. We will again use the same set-up as in Section 6.2, but will vary ϵ in powers of 10, from $\epsilon = 10^{-1}$ down to $\epsilon = 10^{-7}$.

A problem that will arise is that, as with our experiments for source iteration, we are using a direct solve of the transport equation as our benchmark 'true' solution. We define the error at each step of the iteration to be the 2-norm of the difference between

this 'true' solution and the current approximation. However in Section 6.3 we saw an argument why this may be an inaccurate solution for ϵ less that roughly 10^{-5}. Despite this, we will use this benchmark since it remains valid for larger ϵ, and may shed further light on the small-ϵ situation. We will stop iterating once the error has dropped below 10^{-6}. Proceeding with the experiment, we obtain the following table of errors.

Iteration	ϵ						
	10^{-1}	10^{-2}	10^{-3}	10^{-4}	10^{-5}	10^{-6}	10^{-7}
1	5.5e-002	1.6e-003	9.2e-005	3.5e-005	8.9e-006	3.9e-003	3.6e-001
2	5.1e-003	2.2e-003	3.4e-004	2.9e-005	8.0e-007	5.6e-005	3.1e-002
3	8.9e-004	5.1e-004	1.7e-004	1.8e-005		7.2e-005	8.5e-003
4	1.7e-004	1.1e-004	8.2e-005	1.0e-005		5.9e-005	9.7e-003
5	3.1e-005	2.3e-005	3.9e-005	5.7e-006		4.1e-005	1.2e-002
6	6.1e-006	4.8e-006	1.8e-005	3.2e-006		5.9e-005	1.5e-002
7	1.2e-006	1.0e-006	8.4e-006	1.8e-006		8.7e-005	2.3e-003
8	2.4e-007	2.1e-007	3.9e-006	9.9e-007		1.1e-004	6.8e-003
9			1.8e-006			2.1e-004	7.6e-003
10			8.6e-007			8.8e-005	4.5e-003
11						7.0e-005	7.0e-003
⋮						⋮	⋮

Table 6.6: *2-norm of the error in the scalar flux solution found using DSA for various values of ϵ. This uses a direct solve of the transport matrix equation as a benchmark 'true' solution for the errors.*

Table 6.6 shows some expected and some unexpected behaviour. To begin with, it shows a vast improvement in the number of iterations required over vanilla source iteration. The decrease in iterations required from $\epsilon = 10^{-3}$ to $\epsilon = 10^{-5}$ agrees with the fact that the diffusion approximation is more accurate for smaller ϵ. On the other hand, the relatively rapid convergence in the cases $\epsilon = 10^{-1}$ and $\epsilon = 10^{-2}$ was not expected. As we saw in Table 6.3 the scalar flux obtained by transport and diffusion solves disagree by an order of ϵ, and so it is unexpected to convergence in so few iterations for a comparatively large value of ϵ.

If the diffusion equation incurs an error of $O(\epsilon)$, then we might expect to see a faster rate of convergence while the error is bigger than $O(\epsilon)$, then a slower rate of convergence once the error gets smaller that $O(\epsilon)$. In fact we see the error immediately drop to a value in the range of $O(\epsilon)$, and then see slower convergence thereafter. Again, the faster rate of convergence seen for $\epsilon = 10^{-1}$ and $\epsilon = 10^{-2}$ during the later iterations was not expected and is not yet understood.

For $\epsilon = 10^{-6}$ and $\epsilon = 10^{-7}$ we see very poor convergence, which supports our

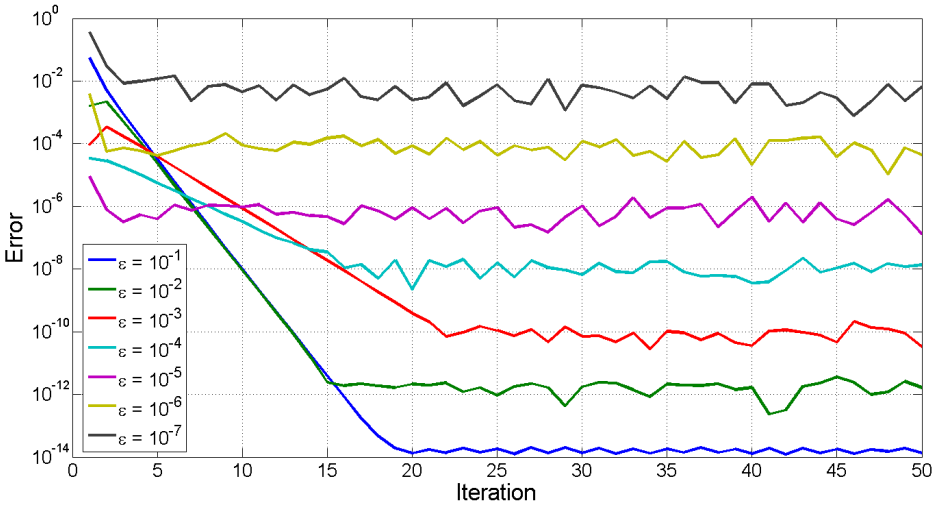

Figure 6-1: *Error stagnation in DSA for several values of ϵ.*

argument at the end of Section 6.3. In Figure 6-1 we allow DSA for every power of ϵ to proceed for 50 iterations, and can observe stagnation of the error in each case. In Section 6.3 it was mentioned that for a value of $\epsilon = 10^{-k}$, we could not expect to improve the accuracy of the solution beyond an error of about $10^{-(16-2k)}$. This can be clearly seen in Figure 6-1.

Following on from this problem, we note that the right hand side of (3.33) also has terms that differ by two orders of magnitude in ϵ. Heuristically as noted above for the transport equation, we would expect this to mean that for very small ϵ, (3.33) would start to behave as if it were in the limit of $\epsilon \to 0$. In the limit, (3.33) simply asserts that

$$0 = \left(\phi^{i+1/2}(\mathbf{r}) - \phi^{i}(\mathbf{r})\right).$$

Therefore, if running our experiment in single precision verifies that the argument in Section 6.3 is correct, then moving to a programming language that can use arbitrary precision should benefit DSA also.

At this stage it would seem sensible to try using a different benchmark as the 'true' solution for evaluating the error. A first idea could be to use a pure diffusion solve (as looked at in Section (6.3)) to find the benchmark scalar flux. We would expect this to work well for smaller ϵ, and have a reasonable idea of its accuracy for each power of ϵ by extrapolating the behaviour in Table 6.3.

One other idea is to use the *method of manufactured solutions*. This involves choosing a neutron flux ψ to be some function of x and μ, which is then substituted into the transport equation. You then work out what function the source term q works out to be to give this flux. Once this is known the transport problem can be posed with that

source, and the solution is then known exactly. We have not done this yet, however it would be a good route to follow as it would allow accurate convergence analysis.

6.5 Conclusions

We have seen numerics that agree with Lemma 2.4 in the 1D case, and also seen how well the diffusion equation approximates the true scalar flux with respect to ϵ. We also identified an issue that arises for very small ϵ, which may be caused by working with too little precision. A way of verifying this was suggested, and if true, a possible solution of working with arbitrary precision was noted. Lastly we looked at DSA and noticed various expected and unexpected behaviours. While working with arbitrary precision might explain some of the behaviour, there are still things that are not understood. These could be caused by flaws in the code, or by misunderstandings in the theory, and further work on this should be high priority for the future.

References

[1] M. Abramowitz and I. A. Stegun. *Handbook of Mathematical Functions.* Dover, 1972.

[2] M. L. Adams and E. W. Larsen. Fast iterative methods for discrete-ordinates particle transport calculations. *Progress in Nuclear Energy*, 40(1):3 – 159, 2002.

[3] R.E. Alcouffe. Diffusion synthetic acceleration methods for the diamond-differenced discrete-ordinates equations. *Nucl. Sci. Eng.;(United States)*, 64(2), 1977.

[4] S. F. Ashby, P. N. Brown, M. R. Dorr, and A. C. Hindmarsh. A linear algebraic analysis of diffusion synthetic acceleration for the Boltzmann transport equation. *SIAM J. Numer. Anal.*, 32:128–178, 1995.

[5] George I. Bell and Samuel Glasstone. *Nuclear Reactor Theory.* Van Nostrand Reinhold Company, 1970.

[6] M. Benzi. Preconditioning techniques for large linear systems: a survey. *Journal of Computational Physics*, 182(2):418–477, 2002.

[7] J. C. H. Blake. Preconditioning of iterative methods for the transport equation. Master's thesis, University of Bath, 2011.

[8] Dan Gabriel Cacuci, editor. *Handbook of Nuclear Engineering, Volume I.* Springer, 2010.

[9] K.M. Case and P.F. Zweifel. *Linear transport theory.* Addison-Wesley series in nuclear engineering. Addison-Wesley Pub. Co., 1967.

[10] J. J. Duderstadt and W. R. Martin. *Transport Theory.* John Wiley and Sons, New York, 1979.

[11] François Golse, Shi Jin, and C. David Levermore. The convergence of numerical transfer schemes in diffusive regimes i: Discrete-ordinate method. *SIAM Journal on Numerical Analysis*, 36(5):1333–1369, 1999.

[12] Anne Greenbaum. *Iterative Methods for Solving Linear Systems.* SIAM, 1997.

[13] G. J. Habetler and B. J. Matkowsky. Uniform asymptotic expansions in transport theory with small mean free paths, and the diffusion approximation. *J. Math. Phys*, 1975.

[14] I. C. F. Ipsen and C. D. Meyer. The idea behind Krylov methods. *Amer. Math. Monthly*, 105(10):889–899, 1998.

[15] Shi Jin and David Levermore. The discrete-ordinate method in diffusive regimes. *Transport Theory and Statistical Physics*, 20(5&6):413–439, 1991.

[16] Shi Jin and David Levermore. Fully-discrete numerical transfer in diffusive regimes. *Transport Theory and Statistical Physics*, 22(6):739–791, 1993.

[17] E. W. Larsen. Unconditionally stable diffusion-synthetic acceleration methods for the slab geometry discrete ordinates equations. Part I: Theory. *Nucl. Sci. Eng.*, 82:47–63, 1982.

[18] Edward W. Larsen. Diffusion theory as an asymptotic limit of transport theory for nearly critical systems with small mean free paths. *Annals of Nuclear Energy*, 7(4-5):249 – 255, 1980.

[19] Edward W Larsen, J.E Morel, and Warren F Miller Jr. Asymptotic solutions of numerical transport problems in optically thick, diffusive regimes. *Journal of Computational Physics*, 69(2):283 – 324, 1987.

[20] E. E. Lewis and W. F. Miller. *Computational Methods of Neutron Transport.* Wiley-Interscience, 1993.

[21] E.E. Lewis and WF Miller. Computational methods of neutron transport. 1984.

[22] Juhani Pitkäranta and L. Ridgway Scott. Error estimates for the combined spatial and angular approximations of the transport equation for slab geometry. *SIAM Journal on Numerical Analysis*, 20(5):922–950, 1983.

[23] A. K. Prinja and E. W. Larsen. *Handbook of Nuclear Engineering, Volume I*, chapter 5. General Principles of Neutron Transport. In Cacuci [8], 2010.

[24] Anthony Ralston and Philip Rabinowitz. *A First Course in Numerical Analysis: Second Edition (Dover Books on Mathematics).* Dover Publications, 2001.

[25] Y. Saad. *Numerical methods for large eigenvalue problems*, volume 158. SIAM, 1992.

[26] Yousef Saad. *Iterative Methods for Sparse Linear Systems, Second Edition.* Society for Industrial and Applied Mathematics, 2003.

[27] Fynn Scheben. *Iterative Methods for Criticality Computations in Neutron Transport Theory.* PhD thesis, University of Bath, 2011.

[28] W.M. Stacey. *Nuclear reactor physics.* Wiley-VCH, 2007.

[29] J.H. Tait. *Neutron transport theory.* Longmans, Green and co. LTD, 1964.

[30] J. S. Warsa, T. A. Wareing, and J. E. Morel. Krylov iterative methods applied to multidimensional S_N calculations in the presence of material discontinuities. *Nuclear Mathematical and Computational Sciences: A century in Review, A Century Anew*, 2003.

Appendix A

A.1 Convergence results for 1D source iteration

In this section we will repeat the analysis presented in Section 2.2 but within a 1D setting. This will follow the same logical progression as the 3D case, and will conclude with a 1D analog of Lemma 2.4.

First of all, we define the one dimensional scalar flux, $\phi(x)$, as you would expect to be

$$\phi(x) = \mathcal{P}\psi(x,\mu), \tag{A.1}$$

with $\mathcal{P}$ defined in (1.15). Now working from the 1D operator form of the transport equation as given in (1.16), source iteration can be defined as

Algorithm 5: Source iteration (1D)

1. Start with some initial $\phi^{(0)}(x)$,
2. solve
$$\mathcal{T}\psi^{(i+1)}(x,\mu) = \sigma_S\phi^{(i)}(x) + Q(x), \tag{A.2}$$
for $\psi^{(i+1)}(x,\mu)$,
3. integrate to find $\phi^{(i+1)}(x) = \mathcal{P}\psi^{(i+1)}(x,\mu)$, and return to step 2.

To obtain a 1D analog of Lemma 2.4, and to understand the error incurred by Algorithm 5, we first give the following two results that are proved in [27] (Lemma 2.3 and Theorem 2.9 respectively).

Lemma A.1:

If $\psi(x,\mu) \in L^2\left([a,b], L^1[-1,1]\right)$ *satisfies*

$$\mathcal{T}\psi(x,\mu) = g(x), \tag{A.3}$$

where $g \in L^2[a,b]$, then

$$\phi(x) = \left(\mathcal{K}_{\sigma_T} g\right)(x) \equiv \left(\mathcal{P}\mathcal{T}^{-1} g\right)(x), \tag{A.4}$$

where $\mathcal{K}_{\sigma_T}$ is defined in [27] (equation (2.15)) and, in 1D, $\mathcal{T}^{-1}$ is defined in [22] (equation (2.2)) and [27] (equation (2.14)).

Theorem A.2:
If $\mathcal{K}_{\sigma_T}$ is the operator used in Lemma A.1 then

$$\|\mathcal{K}_{\sigma_T}\|_{\mathscr{L}(L^2[a,b])} \leq \frac{1}{\sigma_T}. \tag{A.5}$$

Here, $\|\cdot\|_{\mathscr{L}(L^2[a,b])}$ is the standard operator norm defined as

$$\|\mathcal{K}_{\sigma_T}\|_{\mathscr{L}(L^2[a,b])} \equiv \sup\left\{ \frac{\|\mathcal{K}_{\sigma_T} g\|_{L^2[a,b]}}{\|g\|_{L^2[a,b]}} \ : \ g \in L^2[a,b], g \neq 0 \right\} \tag{A.6}$$

Using these results we can state and prove the following:

Lemma A.3:

If $\mathcal{K}_{\sigma_T}$ is the operator used in Lemma A.1 and $\psi(x,\mu) \in L^2\left([a,b], L^1[-1,1]\right)$ satisfies (A.3)*, then*

$$\|\phi\|_{L^2[a,b]} \leq \frac{1}{\sigma_T} \|g\|_{L^2[a,b]}, \tag{A.7}$$

where $\phi(x) = \mathcal{P}\psi(x,\mu)$.

Proof.
The operator norm definition gives

$$\frac{\|\mathcal{K}_{\sigma_T} g\|_{L^2[a,b]}}{\|g\|_{L^2[a,b]}} \leq \|\mathcal{K}_{\sigma_T}\|_{\mathscr{L}(L^2[a,b])} \leq \frac{1}{\sigma_T}. \tag{A.8}$$

Since $\psi(x,\mu) \in L^2\left([a,b], L^1[-1,1]\right)$ satisfies (A.3), we know from Lemma 2.1 that $\phi(x) = \left(\mathcal{K}_{\sigma_T} g\right)(x)$. Thus we have

$$\frac{\|\phi\|_{L^2[a,b]}}{\|g\|_{L^2[a,b]}} \leq \frac{1}{\sigma_T}. \tag{A.9}$$

Multiplying through by $\|g\|_{L^2[a,b]}$ yields the result. □

Subtracting (A.2) from (1.16) leaves the error equation

$$\mathcal{T}e^{(i+1)}(x,\mu) = \sigma_S E^{(i)}(x), \tag{A.10}$$

where

$$\begin{aligned} e^{(i)}(x,\mu) &\equiv \left(\psi - \psi^{(i)}\right)(x,\mu), \\ E^{(i)}(x) &\equiv \left(\phi - \phi^{(i)}\right)(x). \end{aligned} \tag{A.11}$$

We can now state the following result

Lemma A.4:

Under the definitions in (A.11)*, the following bound holds*

$$\left\| E^{(i+1)} \right\|_{L^2[a,b]} \leq \frac{\sigma_S}{\sigma_T} \left\| E^{(i)} \right\|_{L^2[a,b]}. \tag{A.12}$$

Proof.
Combining (A.10) with Lemma A.3 we get immediately

$$\left\| E^{(i+1)} \right\|_{L^2[a,b]} \leq \frac{1}{\sigma_T} \left\| \sigma_S E^{(i)} \right\|_{L^2[a,b]} = \frac{\sigma_S}{\sigma_T} \left\| E^{(i)} \right\|_{L^2[a,b]}. \tag{A.13}$$

□

As in the 3D case, this result proves that source iteration will converge to a solution, however it has the potential to converge very slowly if σ_S/σ_T is close to one.

A.2 Integral equalities for the derivation of the 3D diffusion equation

In this section we will prove two lemmas regarding integral equalities required to complete the derivation of the 3D diffusion equation presented in Section 3.2.

Lemma A.5:

For any $f : V \to \mathbb{R}$, independent of $\Omega \in \mathbb{S}^2$, it holds that

$$\int_{\mathbb{S}^2} \Omega \cdot f(\mathbf{r}) \, d\Omega = 0, \quad \forall \mathbf{r} \in V. \tag{A.14}$$

Proof.
In spherical polar coordinates we have $\Omega = (1, \theta, \varphi)$, with $\varphi \in [0, 2\pi]$ and $\theta \in [0, \pi]$. Define $\tilde{\Omega}$ to be the cartesian equivalent, so

$$\tilde{\Omega} \equiv \begin{pmatrix} \sin(\theta)\cos(\varphi) \\ \sin(\theta)\sin(\varphi) \\ \cos(\theta) \end{pmatrix}. \tag{A.15}$$

A change of variables now gives us

$$\int_{\mathbb{S}^2} \Omega \cdot f(\mathbf{r})\, \mathrm{d}\Omega = \int_{\theta\in[0,\pi]} \int_{\varphi\in[0,2\pi]} \tilde{\Omega} \cdot f(\mathbf{r}) \sin(\theta)\, \mathrm{d}\varphi\, \mathrm{d}\theta. \tag{A.16}$$

Expanding the dot product gives the argument of the integral to be

$$\begin{aligned} \tilde{\Omega} \cdot f(\mathbf{r}) \sin(\theta) = \sin^2(\theta)\cos(\varphi) f(\mathbf{r}) + \sin^2(\theta)\sin(\varphi) f(\mathbf{r}) \\ + \sin(\theta)\cos(\theta) f(\mathbf{r}). \end{aligned} \tag{A.17}$$

Evaluating the integral then immediately gives the result. □

Lemma A.6:

Suppose $f : V \to \mathbb{R}$ is twice continuously differentiable and independent of $\Omega \in \mathbb{S}^2$. Then

$$\int_{\mathbb{S}^2} \Omega \cdot \nabla(\Omega \cdot \nabla f(\mathbf{r}))\, d\Omega = \frac{4\pi}{3} \nabla \cdot \nabla f(\mathbf{r}). \tag{A.18}$$

Proof.
Proceeding in the same way as in the proof of Lemma A.5, a change of variables gives

$$\int_{\mathbb{S}^2} \Omega \cdot \nabla(\Omega \cdot \nabla f(\mathbf{r}))\, \mathrm{d}\Omega = \int_{\theta\in[0,\pi]} \int_{\varphi\in[0,2\pi]} \tilde{\Omega} \cdot \nabla(\tilde{\Omega} \cdot \nabla f(\mathbf{r})) \sin(\theta)\, \mathrm{d}\varphi\, \mathrm{d}\theta. \tag{A.19}$$

Expanding now gives

$$\begin{aligned} &\int_0^{\pi} \int_0^{2\pi} \tilde{\Omega} \cdot \nabla(\tilde{\Omega} \cdot \nabla f(\mathbf{r})) \sin(\theta)\, \mathrm{d}\varphi\, \mathrm{d}\theta \;= \\ &\int_0^{\pi} \int_0^{2\pi} \sin^3(\theta)\cos^2(\varphi)\partial_{xx} f(\mathbf{r}) \qquad + \sin^3(\theta)\sin^2(\varphi)\partial_{yy} f(\mathbf{r}) \\ &\qquad \sin(\theta)\cos^2(\varphi)\partial_{zz} f(\mathbf{r}) \qquad + 2\sin^3(\theta)\cos(\varphi)\sin(\varphi)\partial_{xy} f(\mathbf{r}) \\ &\qquad 2\sin^2(\theta)\cos(\theta)\cos(\varphi)\partial_{xz} f(\mathbf{r}) + 2\sin^2(\theta)\cos(\theta)\sin(\varphi)\partial_{yz} f(\mathbf{r})\, \mathrm{d}\varphi\, \mathrm{d}\theta, \end{aligned} \tag{A.20}$$

where $\partial_{\circledast\circledcirc} \equiv \frac{\partial}{\partial \circledast} \frac{\partial}{\partial \circledcirc}$. Evaluating the various integrals leaves

$$\begin{aligned}\int_0^{\pi}\int_0^{2\pi} \tilde{\Omega}\cdot\nabla(\tilde{\Omega}\cdot\nabla f(\mathbf{r}))\sin(\theta)\,\mathrm{d}\varphi\,\mathrm{d}\theta &= \frac{4\pi}{3}\left(\partial_{xx}f(\mathbf{r})+\partial_{yy}f(\mathbf{r})+\partial_{zz}f(\mathbf{r})\right)\\ &= \frac{4\pi}{3}\nabla\cdot\nabla f(\mathbf{r}).\end{aligned} \tag{A.21}$$

□

A.3 Results from Chapter 4

In this section we prove two results given in Chapter 4. Firstly we prove Lemma 4.2, which says that

Lemma A.7:
If

$$K(z) \equiv \frac{1}{2}\int_a^b \frac{1}{\mu}\exp\left(\frac{-|z|}{\mu}\right)\,d\mu$$

then

$$\int_{\mathbb{R}} K(z)\,dz = b-a.$$

Proof.
Denoting the Fourier transform of K by $\hat{K}$ we have

$$\hat{K}(\xi) = \int_{-\infty}^{\infty}\exp(-2\pi i\xi z)K(z)\,\mathrm{d}z. \tag{A.22}$$

With the definition of K this is

$$\hat{K}(\xi) = \int_a^b\int_{-\infty}^{\infty}\frac{1}{2\mu}\exp(-2\pi i\xi z)\exp\left(\frac{-|z|}{\mu}\right)\,\mathrm{d}z\,\mathrm{d}\mu.$$

Now evaluating this integral we get

$$\begin{aligned}
\hat{K}(\xi) &= \int_a^b \frac{1}{2\mu}\left[\int_{-\infty}^{0} \exp\left(\frac{z}{\mu} - 2\pi i\xi z\right) \mathrm{d}z + \int_0^{\infty} \exp\left(\frac{-z}{\mu} - 2\pi i\xi z\right) \mathrm{d}z\right] \mathrm{d}\mu \\
&= \int_a^b \frac{1}{2\mu}\left[\frac{\exp\left(\frac{z}{\mu} - 2\pi i\xi z\right)}{\frac{1}{\mu} - 2\pi i\xi}\right]_{-\infty}^{0} + \frac{1}{2\mu}\left[\frac{-\exp\left(\frac{-z}{\mu} - 2\pi i\xi z\right)}{\frac{1}{\mu} + 2\pi i\xi}\right]_{0}^{\infty} \mathrm{d}\mu \\
&= \int_a^b \frac{1}{2\mu}\left[\frac{\mu}{1 - 2\pi i\xi\mu}\right] + \frac{1}{2\mu}\left[\frac{\mu}{1 + 2\pi i\xi\mu}\right] \mathrm{d}\mu \\
&= \int_a^b \frac{1}{1 + (2\pi\xi\mu)^2} \mathrm{d}\mu \\
&= \frac{1}{2\pi\xi}\left[\tan^{-1}(2\pi\xi b) - \tan^{-1}(2\pi\xi a)\right]
\end{aligned}$$

Taking a taylor expansion results in

$$\begin{aligned}
\hat{K}(\xi) &= \frac{1}{2\pi\xi}\left(2\pi\xi b - 2\pi\xi a - \frac{(2\pi\xi b)^3}{2} + \frac{(2\pi\xi a)^3}{2} + \dots\right) \\
&= (b - a) + O(\xi^2)
\end{aligned}$$

and so we have that $\hat{K}(0) = (b - a)$. Using this with (A.22) yields the result. □

Next we will prove Lemma 4.3, which says

Lemma A.8 (Fourier Integral Theorem)**:**
Let $f : \mathbb{R} \to \mathbb{R}$, and suppose that f is Lipschitz continuous and also globally bounded by some $\max_\xi |f(\xi)| \equiv C$. Suppose also we have some function $K : \mathbb{R} \to \mathbb{R}^+$ such that

$$\int_{\mathbb{R}} K(z)\ dz = \alpha,$$

where $\alpha \in \mathbb{R}$ is some constant. Then it holds that

$$\lim_{\delta \to 0} \frac{1}{\delta} \int_{\mathbb{R}} K\left(\delta^{-1}(x - y)\right) f(y)\ dy = f(x), \tag{A.23}$$

for all $x \in \mathbb{R}$.

Proof.
First of all, we separate the integral in (A.23) into two parts

$$\frac{1}{\delta}\int_{\mathbb{R}} K\left(\delta^{-1}(x-y)\right) f(y)\,\mathrm{d}y = \overbrace{\frac{1}{\delta}\int_{\mathbb{R}} K\left(\delta^{-1}(x-y)\right) f(x)\,\mathrm{d}y}^{\equiv I_1} + \underbrace{\frac{1}{\delta}\int_{\mathbb{R}} K\left(\delta^{-1}(x-y)\right)\left[f(y)-f(x)\right]\mathrm{d}y}_{\equiv I_2}. \tag{A.24}$$

We will tackle these independently. First of all we consider I_1, and apply a change of variables, $z \equiv \delta^{-1}(x-y)$.

$$\begin{aligned} I_1 &= \frac{f(x)}{\delta}\int_{-\infty}^{\infty} K\left(\delta^{-1}(x-y)\right)\,\mathrm{d}y \\ &= \frac{f(x)}{\delta}(-\delta)\int_{\infty}^{-\infty} K\left(z\right)\,\mathrm{d}z \\ &= f(x) \end{aligned} \tag{A.25}$$

since $\int_{\mathbb{R}} K(z)\,\mathrm{d}z = \alpha$. It therefore remains to prove that $I_2 \to 0$ as $\delta \to 0$. To do this we further separate the remaining integral as follows

$$I_2 = \overbrace{\frac{1}{\delta}\int_{[x-\delta^{\frac{1}{2}},x+\delta^{\frac{1}{2}}]} K\left(\delta^{-1}(x-y)\right)\left[f(y)-f(x)\right]\mathrm{d}y}^{\equiv I_{21}} + \underbrace{\frac{1}{\delta}\int_{\mathbb{R}\setminus[x-\delta^{\frac{1}{2}},x+\delta^{\frac{1}{2}}]} K\left(\delta^{-1}(x-y)\right)\left[f(y)-f(x)\right]\mathrm{d}y}_{\equiv I_{22}}, \tag{A.26}$$

and show that each of I_{21} and I_{22} tends to zero with δ. Considering I_{21} first, we can use the Lipschitz continuity of f (with constant L) to obtain

$$\begin{aligned} |I_{21}| &= \frac{1}{\delta}\int_{x-\delta^{\frac{1}{2}}}^{x+\delta^{\frac{1}{2}}} \left|K\left(\delta^{-1}(x-y)\right)\right| |f(y)-f(x)|\,\mathrm{d}y \\ &\leq \frac{L}{\delta}\int_{x-\delta^{\frac{1}{2}}}^{x+\delta^{\frac{1}{2}}} K\left(\delta^{-1}(x-y)\right)|y-x|\,\mathrm{d}y. \end{aligned} \tag{A.27}$$

Noting that $|y-x| \leq \delta^{\frac{1}{2}}$ and applying the same change of variables as before we get

$$\begin{aligned} |I_{21}| &\leq \frac{L\delta^{\frac{1}{2}}}{\delta}(-\delta)\int_{\delta^{-\frac{1}{2}}}^{-\delta^{-\frac{1}{2}}} K(z)\,\mathrm{d}z \\ &= L\delta^{\frac{1}{2}}\int_{-\delta^{-\frac{1}{2}}}^{\delta^{-\frac{1}{2}}} K(z)\,\mathrm{d}z. \end{aligned} \tag{A.28}$$

Since $\delta^{\frac{1}{2}} \to 0$ as $\delta \to 0$, we have that $I_{21} \to 0$ also.

Now to show that $I_{22} \to 0$ with δ we split our integral one last time as

$$I_{22} = \overbrace{\frac{1}{\delta}\int_{x+\delta^{\frac{1}{2}}}^{\infty} K\left(\delta^{-1}(x-y)\right)[f(y)-f(x)]\,\mathrm{d}y}^{\equiv I_{22}^{+}} + \underbrace{\frac{1}{\delta}\int_{-\infty}^{x-\delta^{\frac{1}{2}}} K\left(\delta^{-1}(x-y)\right)[f(y)-f(x)]\,\mathrm{d}y}_{\equiv I_{22}^{-}}. \tag{A.29}$$

Now using the global maximum of f and applying the same change of variables, we proceed as follows

$$\begin{aligned} \left|I_{22}^{+}\right| &\leq \frac{2C}{\delta}\int_{x+\delta^{\frac{1}{2}}}^{\infty} K\left(\delta^{-1}(x-y)\right)\,\mathrm{d}y \\ &= \frac{2C}{\delta}(-\delta)\int_{-\delta^{-\frac{1}{2}}}^{-\infty} K\left(z\right)\,\mathrm{d}z \\ &= 2C\int_{-\infty}^{-\delta^{-\frac{1}{2}}} K(z)\,\mathrm{d}z. \end{aligned} \tag{A.30}$$

Since $-\delta^{-\frac{1}{2}} \to -\infty$ as $\delta \to 0$, this tells us that $I_{22}^{+} \to 0$ with δ too.

Similarly for I_{22}^{-} we find that

$$\left|I_{22}^{-}\right| \leq 2C\int_{\delta^{-\frac{1}{2}}}^{\infty} K(z)\,\mathrm{d}z, \tag{A.31}$$

which also goes to zero with δ. Thus the result holds. □